

GEOLOGICAL SURVEY OF CANADA  
OPEN FILE 2015

**STUDIES IN THE STERRETT MINE AREA,  
EASTERN TOWNSHIPS, QUEBEC**

This document was produced  
by scanning the original publication.

Ce document a été produit par  
numérisation de la publication originale.

**W.E. Trzcienski, Jr.**

Contribution to the Federal Asbestos Initiatives Geoscience Research Program,  
1984-87



Energy, Mines and  
Resources Canada

Énergie, Mines et  
Ressources Canada

**Canada**

GEOLOGICAL SURVEY OF CANADA  
OPEN FILE 2015

**STUDIES IN THE STERRETT MINE AREA,  
EASTERN TOWNSHIPS, QUEBEC<sup>1</sup>**

**W.E. Trzcienski, Jr.<sup>2</sup>**

- 1 Contribution to the Federal Asbestos Initiatives Geoscience Research Program  
1984-87, Contract 23233-6-0312101-ST
- 2 Département de Géologie, Université de Montreal, Montreal, Québec, H3C 3J7

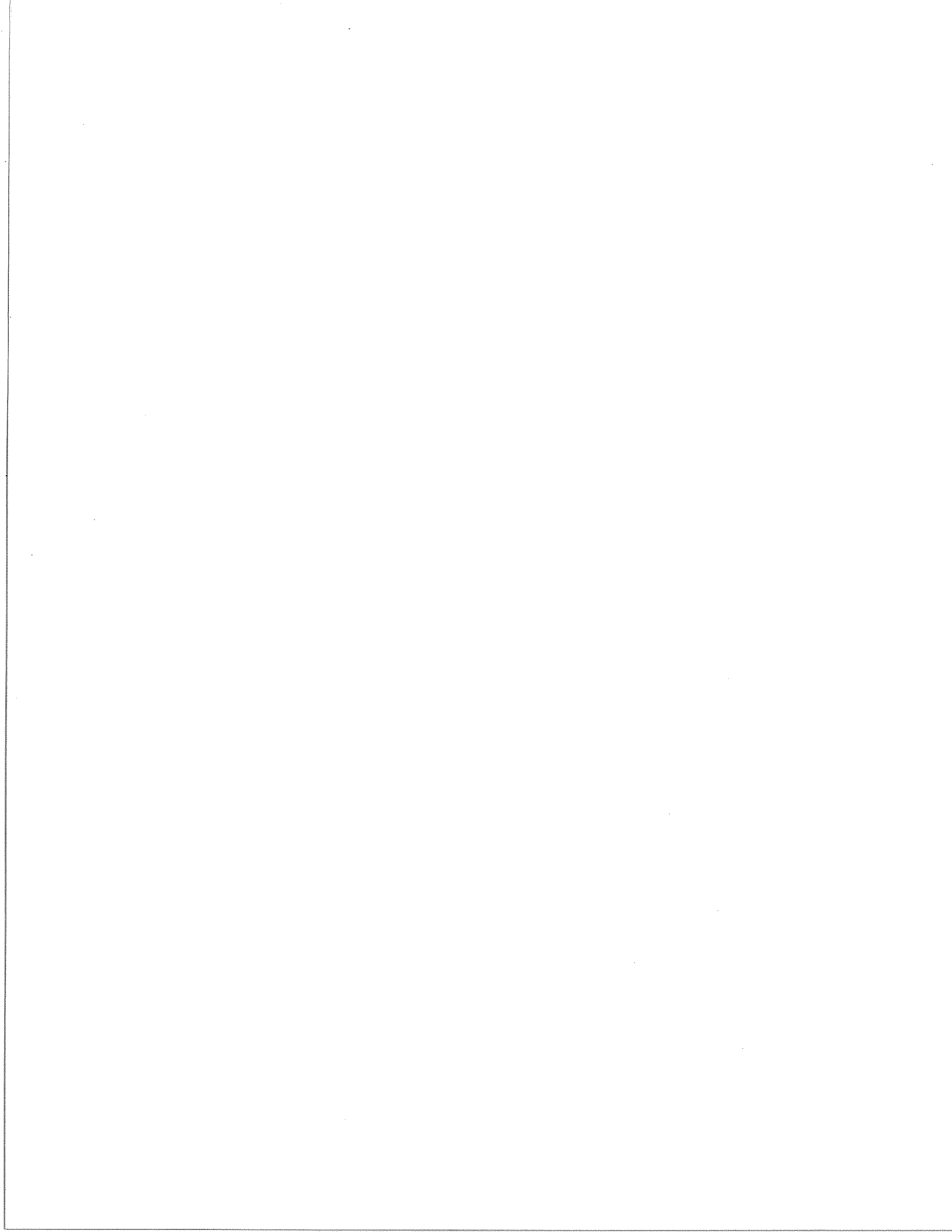
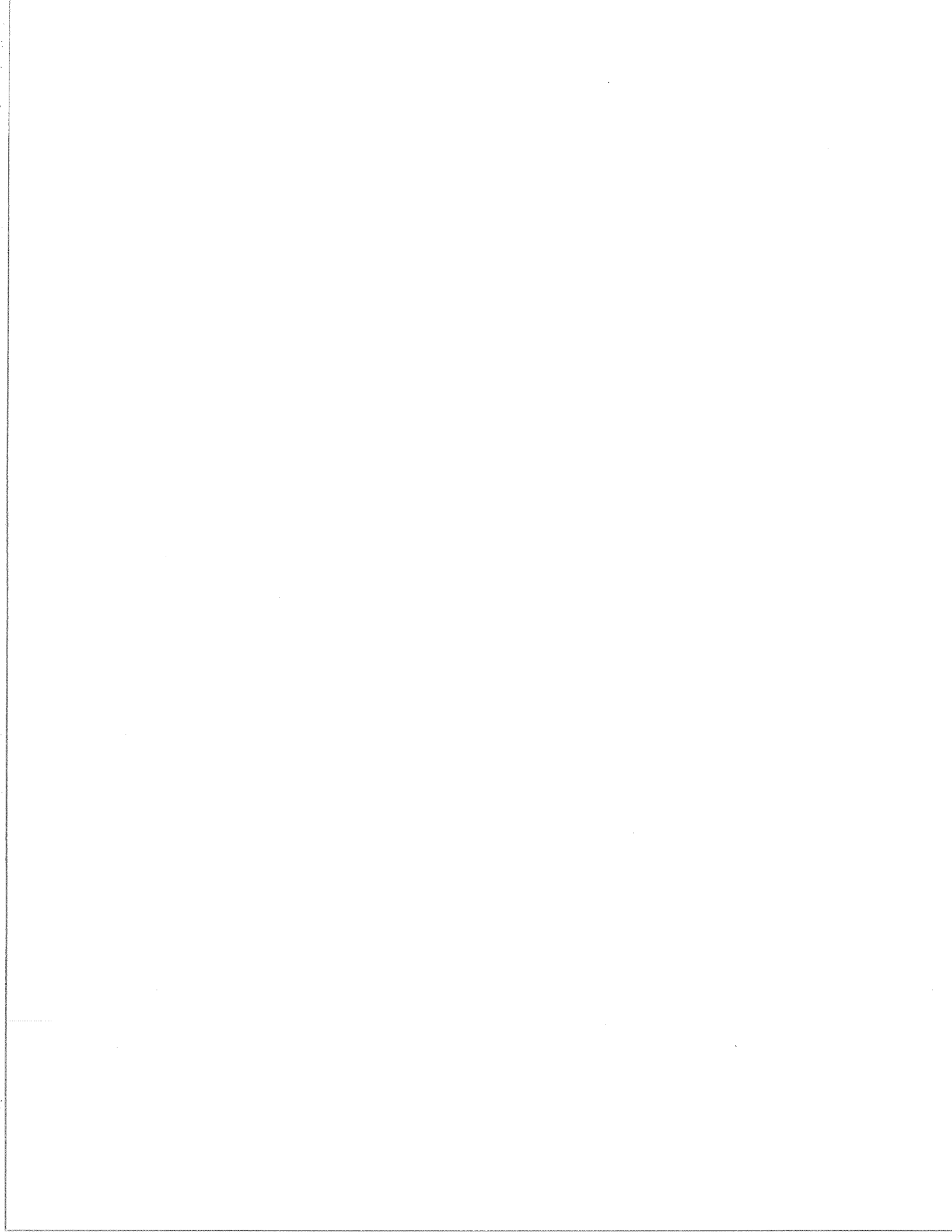


## TABLE OF CONTENTS

INTRODUCTION .....	1
LOCATION AND ACCESS .....	1
REGIONAL GEOLOGIC SETTING .....	1
PREVIOUS WORK AT THE STERRETT PROPERTY .....	3
FIELD INVESTIGATIONS .....	4
PETROGRAPHY .....	11
MINERALOGY AND MINERAL CHEMISTRY .....	14
Serpentine .....	16
Chromite .....	16
Chlorite .....	22
Olivine .....	22
Magnetite .....	22
Sulphides .....	22
Clinopyroxene .....	25
Amphibole .....	25
Mn-Ilmenite-Pyrophanite .....	25
Garnet .....	25
Feldspar .....	28
Calc-Silicate Minerals .....	28
GEOCHEMISTRY .....	28
PETROGENESIS .....	33
Igneous History .....	33
Metamorphic History .....	34
CONCLUSIONS .....	38
ACKNOWLEDGEMENTS .....	38
REFERENCES .....	39
APPENDIX I           : Microprobe analyses of minerals from the Sterrett Chromite Mine area	
APPENDIX II         : CIPW norm calculated from analyses presented in Table 13	



## INTRODUCTION

Chrome spinel is one end member of the spinel family of minerals that also includes hercynite, picrochromite, magnesioferrite and magnetite. Chrome spinel shows great compositional variability because of the solid solution that exists toward the other endmember compositions. For the purposes of this study, this Cr-dominant spinel mineral of varying composition will simply be called chromite.

Chromite is ubiquitous as disseminated grains in rocks of the Quebec ultramafic belt which extends from the Quebec-Vermont border in the south, to the eastern end of the Gaspé Peninsula in the north. In these same rocks, chromite is also found less commonly as concentrated lenses or pockets. It is in these latter concentrations that minerals of composition nearer the endmember chromite are found, and which, in the past have been mined for their chrome content. One such exploitation is the former Sterrett Chromite Mine at St. Cyr in the Eastern Townships, Quebec.

This report presents work done during the summer of 1986 and the winter of 1986-1987 on rocks found in and around the former Sterrett Mine, and endeavors to characterize the geological setting of the chromite deposit, to describe the chrome-bearing ore and associated rocks and to use developed concepts as exploration tools in searching for other, as yet uncovered, chromite-bearing deposits.

## LOCATION AND ACCESS

The Sterrett Chromite Mine is 13 km north of the town of Richmond, which is located on the St. Francois River in the Eastern Townships, Quebec (Fig. 1). To reach Richmond one can travel northwestward from Sherbrooke or southeastward from Drummondville along Quebec Autoroute 55. Rte 116 which passes north-south through Richmond is a second access route to the area and leads to Quebec City in the north and to Acton Vale in the south. To reach the mine site, which is found on Lots 7,8,9 and 10, Range X, Cleveland Township, Richmond County, one travels east from Le Centre d'Achat in Richmond along a secondary road toward St. Cyr and turns onto the mine road just before Greenshields. As the former mine site is presently a test site for CIL explosives, a locked gate blocks access to the main mine area by motor vehicle. Entrance to the mine site itself should be requested from M. Marc Lessard at CIL (467-3382 local 2094). Local topography, roads and mine site location are all marked on the 1:50,000 NTS topographic sheet 31H/9 - Richmond, Quebec.

## REGIONAL GEOLOGIC SETTING

The Sterrett property occurs within the ultramafic belt of the Quebec Appalachians, which also hosts other exploited chromite occurrences. The ultramafic rocks (Fig. 2) form a more or less continuous belt that is bounded on the west by the Caldwell Formation (St.-Julien and Hubert, 1975) and the Oak Hill Group (Marquis, 1986). To the east the bounding rocks are part of the St Daniel Formation (St.-Julien and Hubert, 1975). Within the ultramafic belt, there are also gabbros and mafic volcanics along with crosscutting felsic rocks that vary compositionally from granite to tonalite (Fig. 2). Disseminated chromite is found throughout the ultramafic rocks but massive chromite is much less common. Early interpretation of the ultramafic rocks was that they represented a sill intruded into the country rocks (Cooke, 1950). In light of plate tectonic models a more recent interpretation is that these rocks are part of a late Ordovician obducted ophiolite complex originally generated in early to middle Ordovician time as part of the Iapetus ocean floor (St.-Julien and Hubert, 1975).

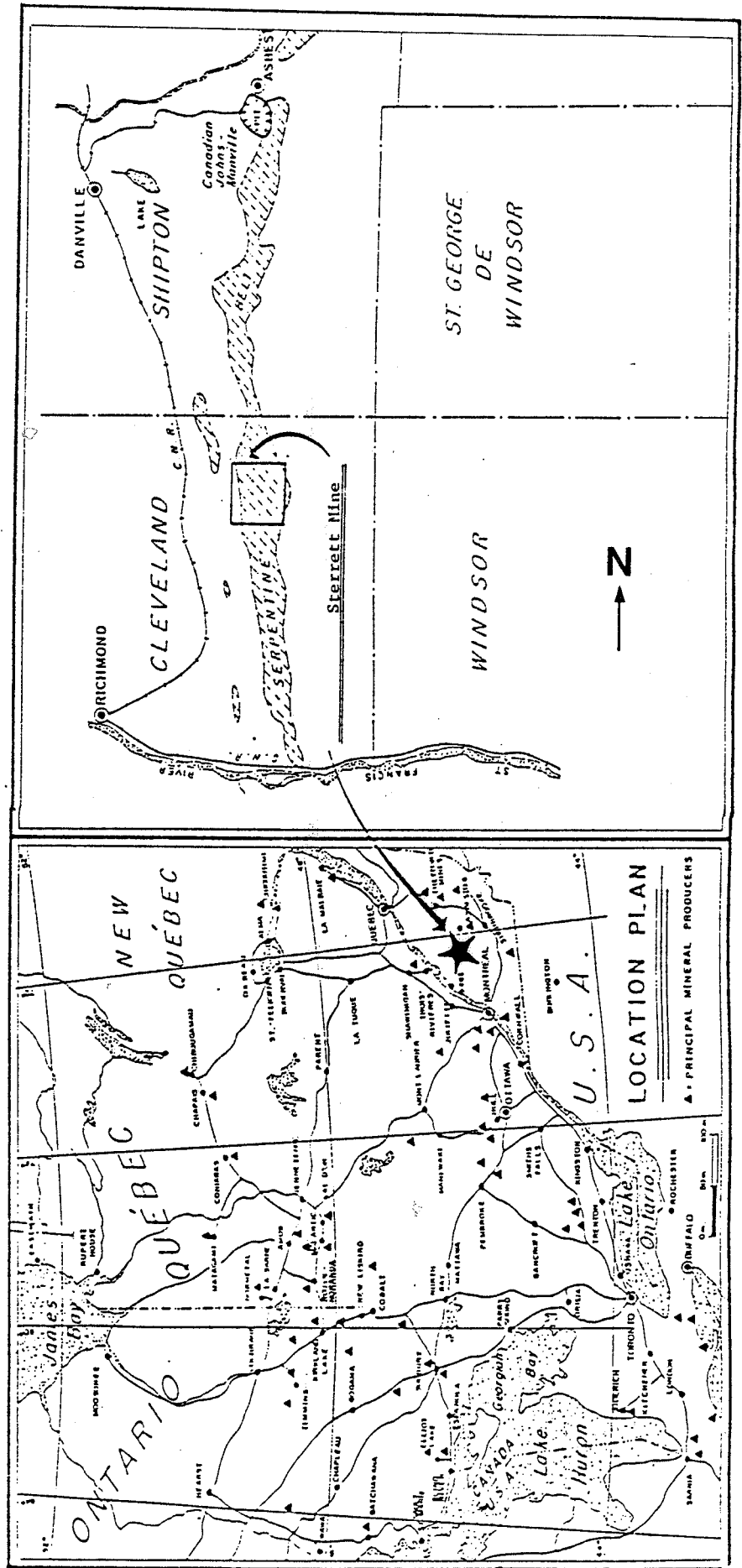


Figure 1 General location map of the Sterrett Mine

## PREVIOUS WORK AT THE STERRETT PROPERTY

The exploration for and exploitation of chromite in the Quebec ultramafic belt began in the latter part of the 19th century (Dennis, 1932). The first references to chromite in this area occur at midcentury in reports of the Geological Survey for the years 1846, 1847 and 1848.

The first shipments of ore were in 1861 from South Ham Township in Wolfe County. It was some 25 years later, however, before significant quantities of ore were shipped. The peak production was reached in 1906 with a majority of the ore coming from Coleraine Township south of Thetford Mines. With the onset of World War I and shipments of ore from South Africa imperiled, exploitation of Quebec chromite resumed.

In 1916 Mr. D.B. Sterrett formed the Quebec Asbestos and Chrome Company to mine the chromite at a property near St. Cyr, Quebec (Dennis, 1932). In 1917, over 9,000 tons of ore were extracted, and the following year Sterrett moved a mill onto the site to process the ore locally. Nearly 6,000 tons of ore were shipped in 1918. Also during that year, underground mining commenced from a shaft sunk to the 196 foot level, with drifts at 109 and 184 feet. At the 109 foot level, some 67 feet from the shaft, chromite was intersected that extended 100 feet to the south where it pinched out; 75 feet of drifting to the north remained in massive ore. With the end of World War I the South African supplies were again less expensive to obtain and chromite mining in the Eastern Townships ceased.

With the onset of World War II, Quebec chromite again became a marketable commodity. From 1940-1942, some 85 chromite deposits were investigated by the Geological Survey of Canada (Stockwell, 1944). Deposits in operation had a total mill capacity of 750 tons per day. During this period the property, now called the Sterrett Mine, was operated by Chromite Ltd. A mill with a capacity of 150 tons per day was put into operation in 1942. The old operations of WWI were reopened, and the 184 foot level drift was extended to 1170 feet along the ore zone. Three new, deeper levels were also opened, at 280, 380 and at 480 feet. From 1942 to 1945 approximately 100,000 tons of ore were extracted from the Sterrett Mine. At this time, C.H. Stockwell and J.W. Ambrose mapped in great detail (scale 1" = 20') the belt of high chromite content rocks in the immediate mine area.

With the end of WWII, Quebec chromite was again displaced by that from foreign sources. In 1951, Ascot Metals carried out 1700 meters of drilling with positive indications. This was followed in 1955 by a magnetic survey and a further 1200 m of drilling by National Gypsum (Canada). The last major exploration on the property was done in 1972 by Pathfinder Resources. Their major interest was asbestos fiber found in peridotite west of the major chromite-bearing belt. During this evaluation, 72,000 feet of core were taken indicating only minor amounts of chromite in the area of high asbestos content. Watts, Griffis and McQuat, who carried out the evaluation for Pathfinder, concluded that an economic feasibility study was necessary before initiation of an exploration program for chromium (Mullins and McQuat, 1976). Most recently, Nokomis Resources Inc. laid claim to the property and carried out some preliminary work in 1985. Since then, Nokomis Resources has been absorbed by Gateford Resources which is now undertaking an exploration program.



## FIELD INVESTIGATION

Six weeks were spent at the Sterrett Mine site and surrounding area during June and July, 1986. The detailed geologic map of Ambrose and Stockwell (A&S) was used as a base map. Re-establishment of the A&S (Fig. 3) baseline was easily done as all the steel pins marking this line are still in place. In addition a number of drill holes shown on their map were also relocated from drill casings that are also in place. Vegetation and mine tailings have covered a number of the outcrops shown on the A&S map, but where outcrop is still available the A&S map was true to the geology observed. This map in reduced form (Fig. 4), serves as a point of reference for discussions that follow as well as a location map for samples taken for laboratory examination.

The Eastern Townships ultramafic belt in which the chromite deposits are found is interpreted as a piece of obducted ocean floor (St.-Julien and Hubert, 1975). As such, much of the tectonic structure and post igneous recrystallization has been assigned to the obduction process (St.-Julien and Hubert, 1975). The regional trends of serpentinite foliation and the chromite-rich horizons are essentially colinear at N25-30° E and vertical dip. Although local, well-polished slickensided surfaces commonly found in the ultramafic rocks suggest intense deformation, the colinearity of the numerous chromite pits at the Sterrett property (Fig. 4) over a 500 meter distance indicates that the deformation did not produce major displacements between adjacent blocks in this area. Fiber-growth zones on slickensided surfaces (Fig. 5) suggest, from the Durney-Ramsay (1973) model of incremental strain measured from growth fibers, a maximum displacement on the order of two meters or less subparallel to the regional foliation. The map pattern and field relations also show a minor left-lateral, steeply dipping fault set that on any one fault has movement commonly less than 3 meters. Exposed at the south end of Pit B is a small left-lateral splay fault that is defined by a talc zone. The well developed schistosity-cleavage relationship in the zone (Fig. 6) demonstrates the relative movements of adjacent blocks - the strike movement is left-lateral and the dip movement is 45° to the south.

The pits from which the chromite was mined at the surface are bounded by vertical walls. As mentioned above, local displacement during tectonic deformation was not great and a major part of the strain was probably taken up in the flow of soft serpentine around the more competent chromite layers. Evidence of movement parallel to the major foliation is to be found in thin chromite beds where clots of massive chromite are rotated and brittlely fractured producing spiral-like tails of disseminated chromite on either side of the rotated clot (Fig. 7). Late-stage block fracturing of massive chromite occurred on relatively shallow-dipping conjugate fault sets and can be seen in most of the mined pits. A stereonet analysis (Fig. 8) of one of these conjugate sets indicates that the major structural compression direction is oriented SE-NW with an extensional component in the vertical direction. A plot of a number of poles of striations on slickensided surfaces (Fig. 9) also supports this general SE-NW direction of movement, which is also postulated as the direction of transport during obduction (St.-Julien and Hubert, 1975). This style of deformation gives rise to the general fracture pattern sketched in Fig. 10 and which is shown schematically for a conjugate set in Fig. 11. These block diagrams portray a shortening produced in a near horizontal direction and extension in the vertical direction, a model that mirrors the structure observed at Sterrett.

The vertical orientation of the chromite-rich band is further confirmed by the drilling program carried out by Pathfinder Resources. Drilling of vertical holes, some to a depth of 400 feet on either side of the chromite-rich band encountered only serpentine with minor disseminated chromite. One exception (hole 33, Fig. 12) intersected massive chromite but only across an interval of several centimeters. Old

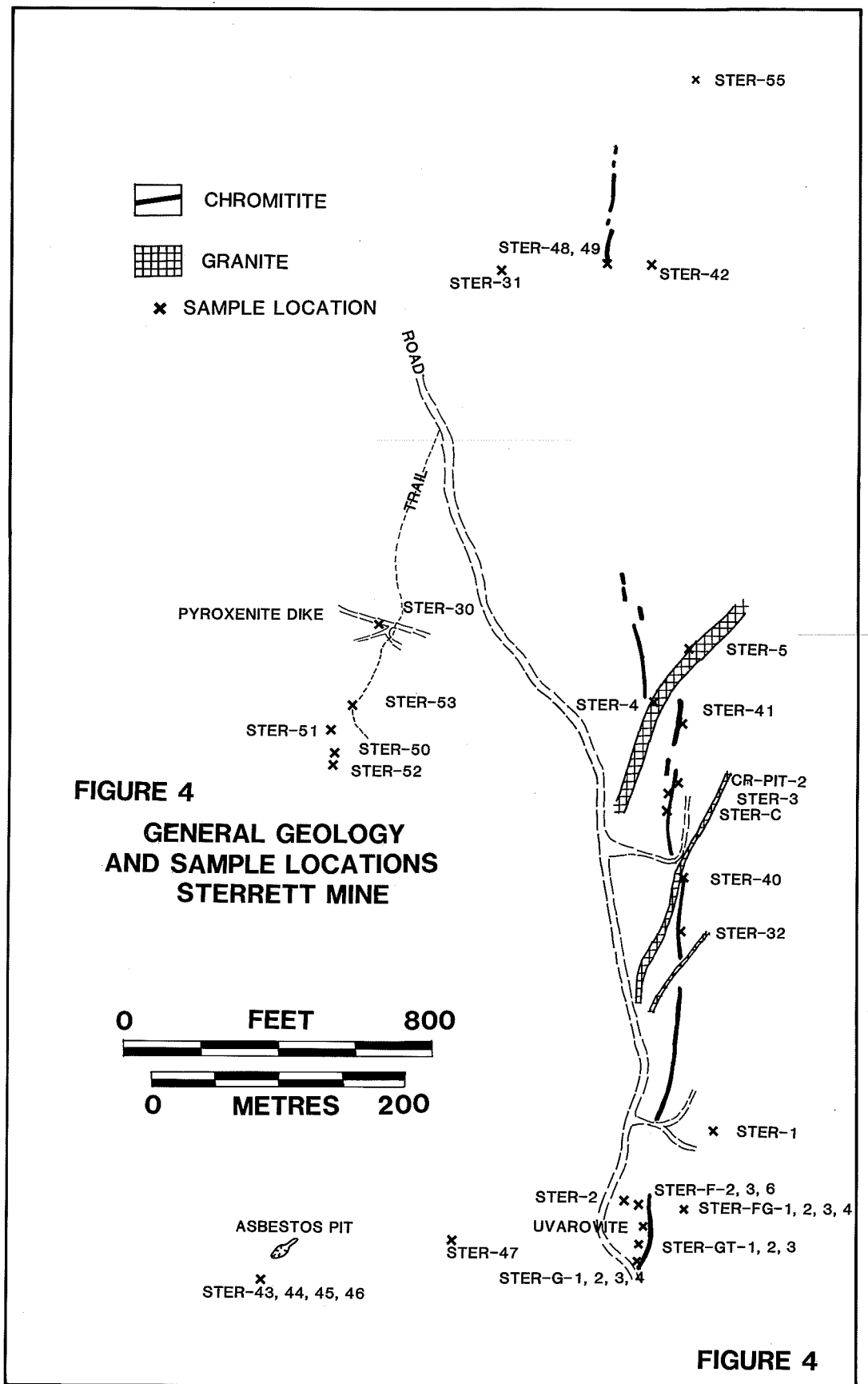




FIGURE 5 : Chrysotile fiber growth on a slickensided surface at Pit C (FIGURE 4). Note the two orientations of fiber growth.



FIGURE 6 : Schistosity-cleavage relationship displayed in a fault zone containing talc. The left wall (west) is granite and to the right of the talc zone is massive chromite. The relative movement sense is that the massive chromite has moved up and northward relative to the left wall (from SE corner of Pit B).

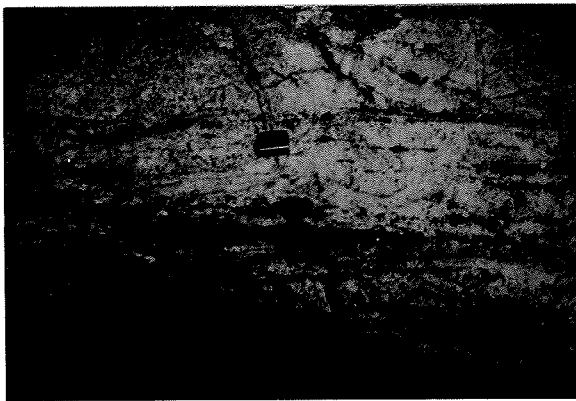


FIGURE 7 : Chromite-rich layer that has been deformed brittlely giving rise to a sigmoidal train (below magnet) of chromite fragments broken from a large nodule of chromite (from Pit A).

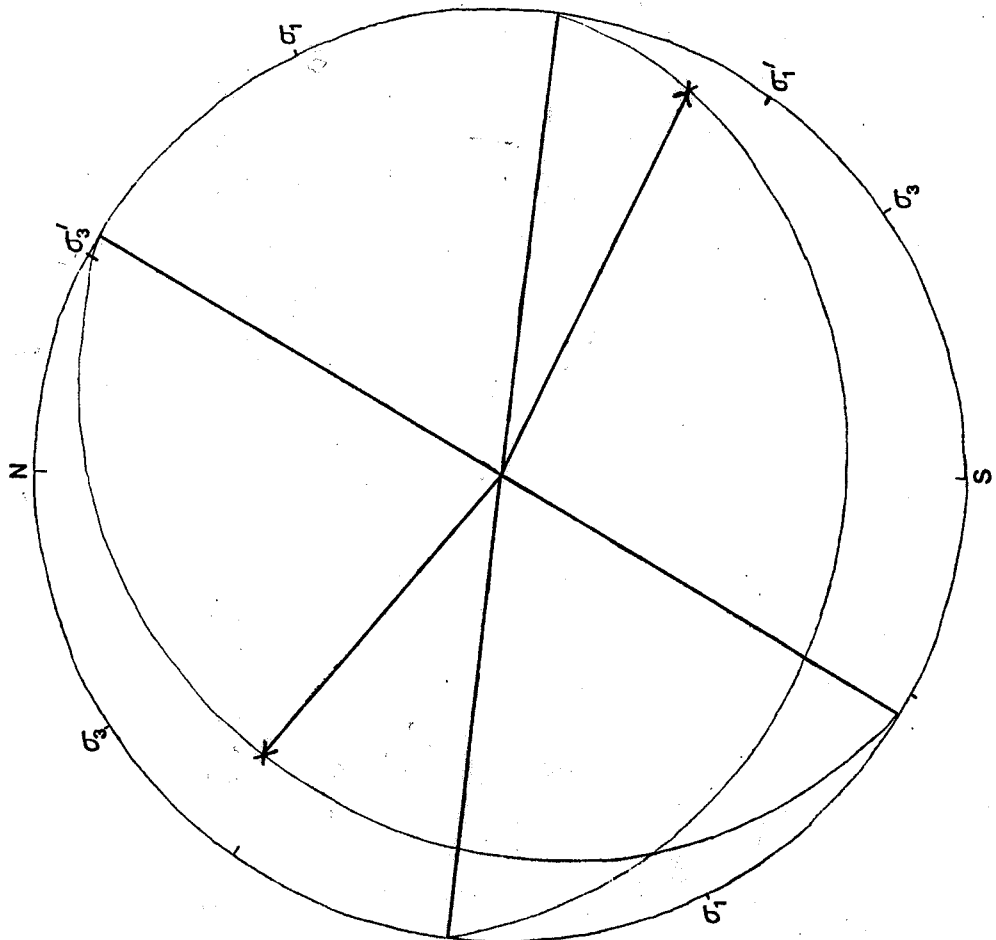


FIGURE 8: A stereonet analysis of a conjugate fault set (at Pit B) typical of shallow dipping faults in the Sterrett area.  $\sigma_1$  is defined as the direction bisecting the acute angle between the fault planes. The true direction of maximum stress ( $\sigma_1'$ ) is found by the method of Arthaud (1969), which in this case is S55 E.

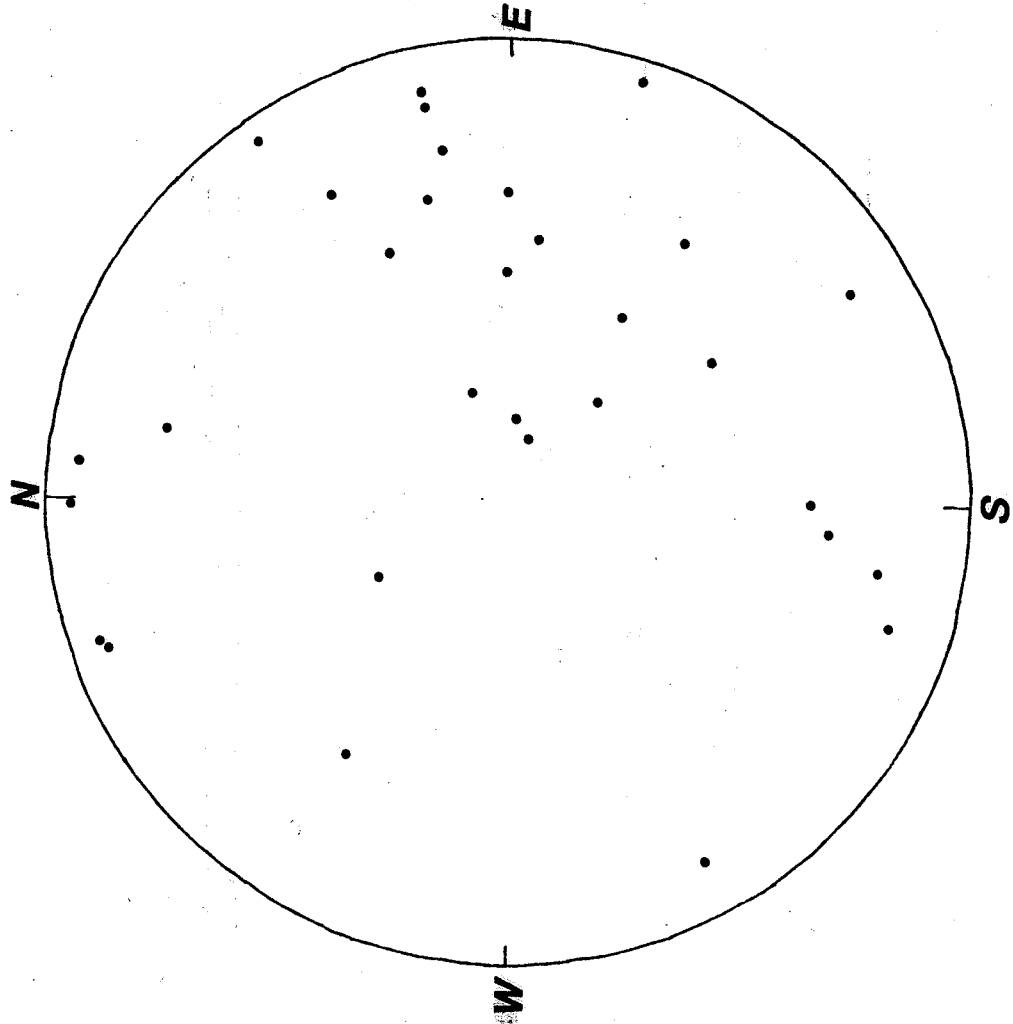


FIGURE 9: A stereonet plot of a number of poles of striations found on slickensided fault surfaces in the Sterrett area. A south-east to northwest sense of movement is indicated.

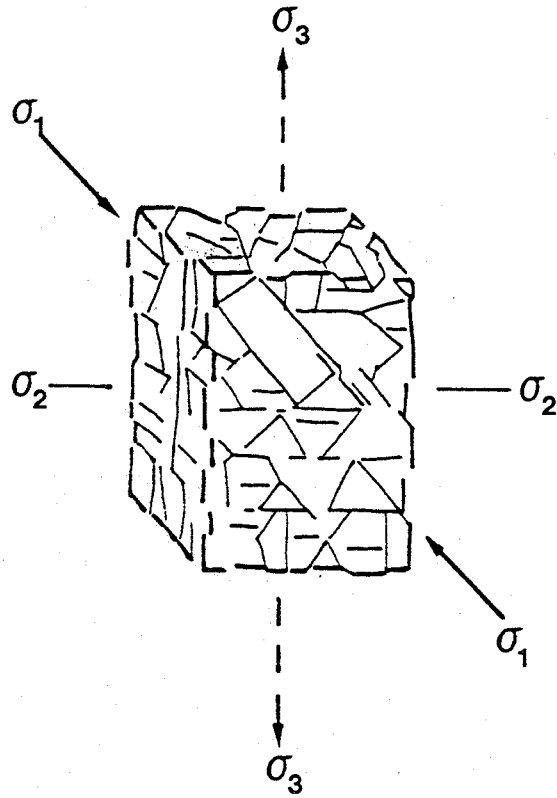


Figure 10: A schematic representation of deformation of an original cubic block due to directed orthogonal stresses.

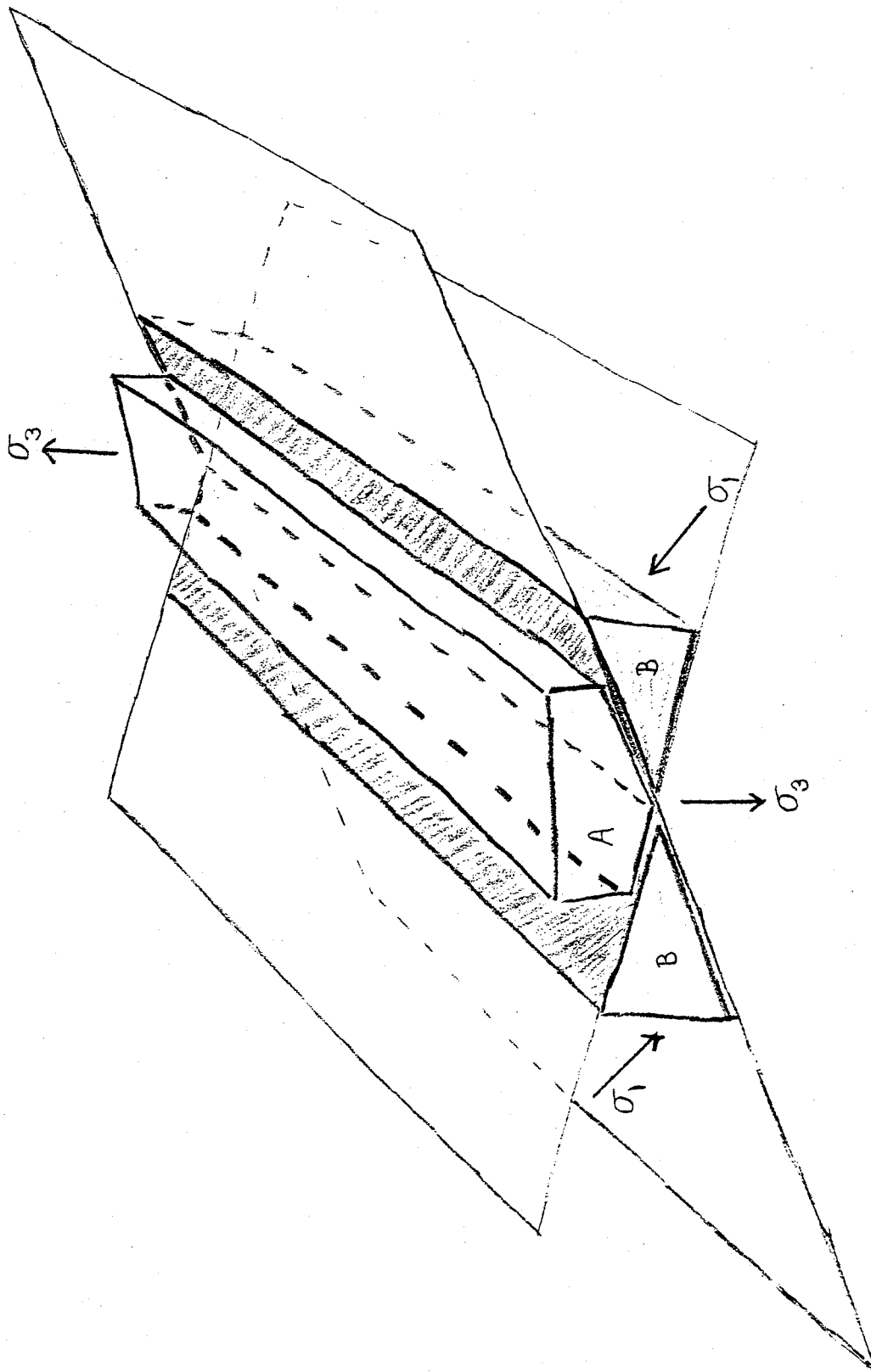


Figure 11: Schematic block movement relative to the maximum ( $\sigma_1$ ) and minimum ( $\sigma_3$ ) stress directions on a conjugate fault set.

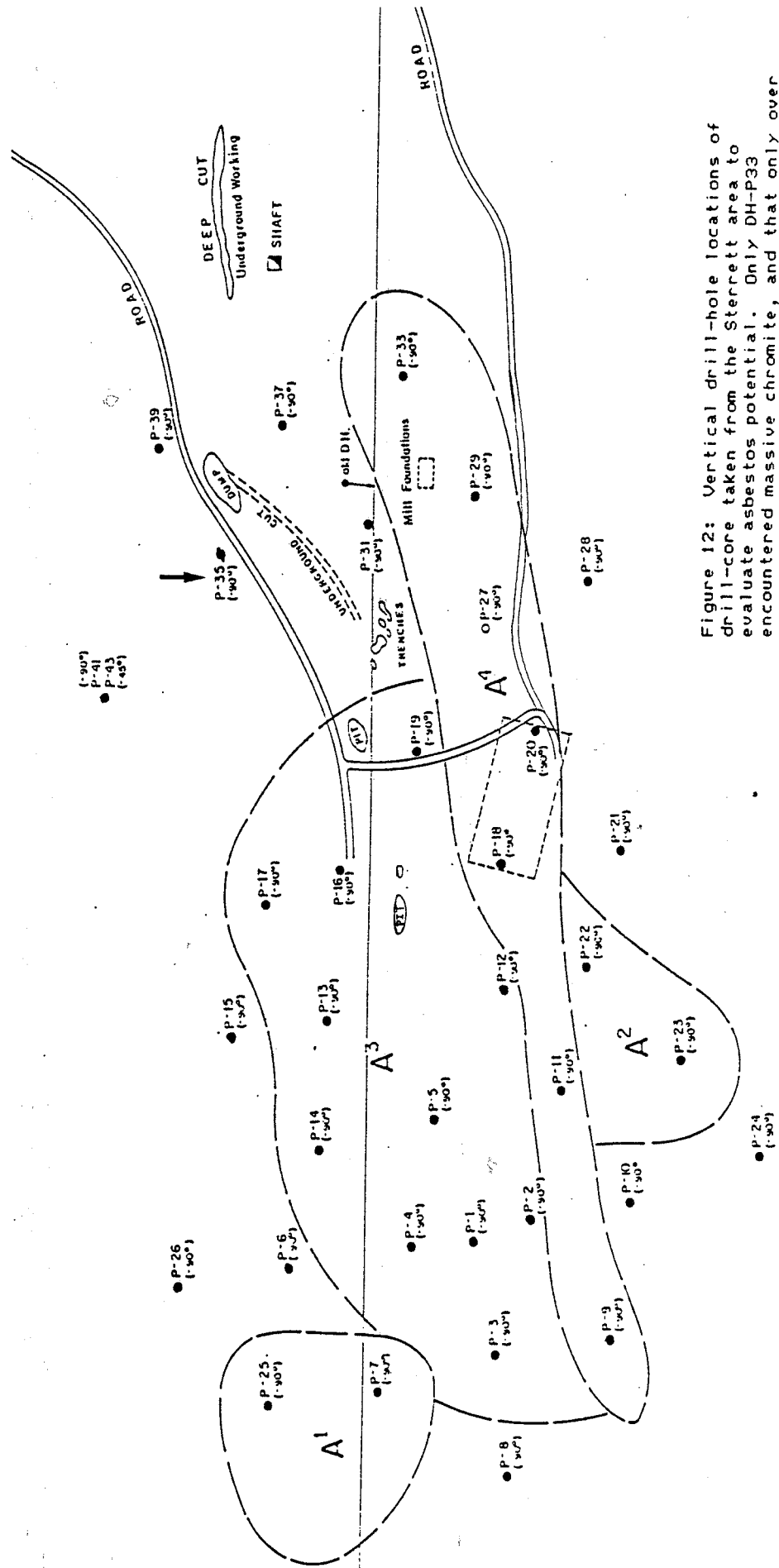


Figure 12: Vertical drill-hole locations of drill-core taken from the Sterrett area to evaluate asbestos potential. Only DH-P33 encountered massive chromite, and that only over an interval of less than 5cm.

mine records (Jerrom, 1951) of the underground operations to a depth of 500 feet also indicate that the chromite was found in a narrow band, and drifting away from this band always encountered barren serpentine.

The rocks enclosing the chromite rich horizon are also fractured similarly to the chromite-rich band. Massive blocks of serpentized peridotite and dunite are commonly bounded by slickensided fault surfaces. As in the chromite layers, total displacement is not large and commonly one can correlate, across fault planes, blocks that were originally continuous.

The massive peridotite is characterized by large serpentine and/or bastite platelets (Fig. 13) that pseudomorph the original olivine and pyroxene. In fracture zones of the peridotite one commonly observes microlayers of asbestos, but immediately next to the fracture the peridotite retains much of its pseudomorphed igneous texture (Fig. 14). The serpentized dunite, which is the most common host to the massive chromite, is characterized by irregularly shaped, subparallel, black laminations of dust-size magnetite particles in an olive-green matrix of serpentine after olivine. This "mackerel striping" (Fig. 15) is produced by the expulsion of Fe from the igneous silicates during the serpentization process. This dunite stands in sharp contrast to the peridotite described above, and serves as a good marker in searching for chromite-rich layers. The two rock types are commonly interlayered (Fig. 16) parallel to the regional foliation and chromite-rich layers. This parallelism suggests that the original igneous rocks were part of a layered sequence.

Further evidence that supports the concept of an originally layered igneous sequence is the presence of thin ( 5 cm), white bands (Fig. 17) between layers of chromite, found at a number of the pit excavations. Mineralogy and chemistry of a particularly thick (>1 m) white layer found in Pit G (Fig. 18) suggests that these bands were originally anorthosite layers in the sequence. The foliated ultramafic rocks are cut by late-stage, fine-grained pyroxenite dikes that vary in thickness from a few centimeters to 50 centimeters. Although these dikes do not show a strong preferential orientation the majority have an east-west axis rather than a north-south one. The only other rock type recognized at Sterrett is what can be broadly called a granite. In outcrop the rock is light-colored and is comprised of quartz, feldspar, biotite and commonly a sulphide. Several of these larger granite bodies cut across (Fig. 4) the regional foliation and ultramafic layering. In Stockwell's (1944) cross-section, based on mapping the underground workings, these granite bodies are seen to plunge southward, and appear to be related to the general tectonic transport direction discussed above. The association of granite in ultramafic rock is not unique to the Sterrett property, as similar associations are found throughout the Eastern Townships ultramafic belt.

## PETROGRAPHY

A total of 125 thin sections, polished thin sections and polished sections were examined. The most common ultramafic assemblage contains serpentine (most common is antigorite - confirmed by x-ray diffraction - with chrysotile fiber less common), chromite and minor carbonate. The ratio of chromite to serpentine is variable with one or the other predominating in the assemblage; however, high serpentine content is generally the rule. Where serpentine is the major phase, it occurs either as a mesh-like network, that pseudomorphs large igneous silicates, or as a cross-hatched intergrowth of acicular grains. Chromite in these serpentine-rich rocks is generally euhedral and shows little to no brittle fracturing (Fig. 19). Carbonate, usually magnesite, is more common in the chromite-poor rocks than in





FIGURE 13 : Coarse-grained peridotite indicating little to no deformation (locality FG, FIGURE 4).



FIGURE 14 : Fractured coarse-grained peridotite with fracture fillings of microlayers of chrysotile asbestos (from west side of Pit F).



FIGURE 15 : "Mackerel striping" common to serpentinized dunite associated with chromitite (locality FG, FIGURE 4).



FIGURE 16 : Layer of "mackerel striped" dunite (center of photo) enclosed within layers of fine-grained peridotite (from north end of Pit B).



FIGURE 17 : Thin, altered meta-anorthosite layer sandwiched between two chromitite layers (sample is 8 X 15 cm, from Pit-G).



FIGURE 18 : Large band of meta-anorthosite in contact (under pencil) with serpentinized chromitite (from Pit-G).

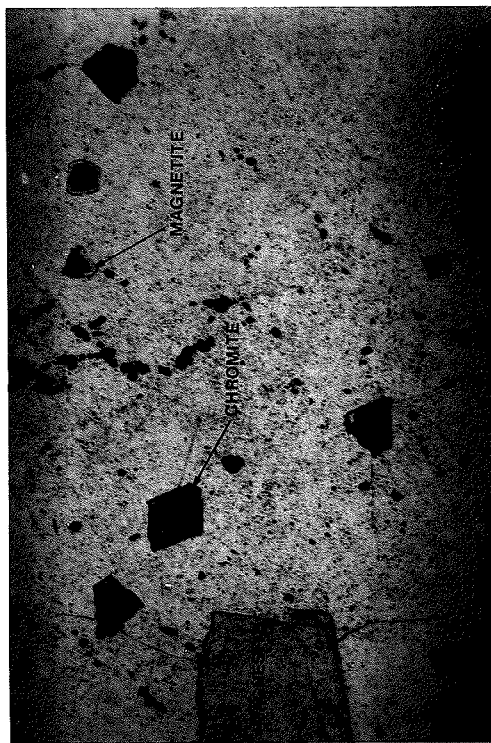


FIGURE 19 : Euhedral, disseminated chromite grains surrounded by atoll-like magnetite. The small black grains in the matrix are also magnetite. The large refringent grain to the left of the photo is magnesite, and the matrix is antigorite (the field of view is 3mm wide).

the chromitites (>50% chromite). Magnetite, as minute grains, is ubiquitous in these rocks and in some serpentinites, the sulphide heazlewoodite is present.

Commonly the chromitites are in sharp contact with the surrounding rock (Fig. 20). In several places graded igneous bedding is observed, which in all observed cases indicates igneous, stratigraphic tops to the west. The spinel phase of chromitites is deep red in color and is generally rounded in shape with numerous embayments of serpentine. Brittle fracturing varies from minor breakup of the grains (Fig. 21) to extensive fracturing (Fig. 22). Where chromite is not extensively fractured, relict olivine is commonly observed as 5-50  $\mu$ m rounded inclusions (Fig. 21).

The layers interpreted to be anorthositic in origin contain two principle assemblages. The thin layers are cut by fractures perpendicular to the layering along which chlorite has grown. The remainder of the assemblage in decreasing percentage of minerals consists of prehnite and grossular as the major phases and then pumpellyite, zoisite, plagioclase and a barium-bearing K-feldspar replacing plagioclase. The second assemblage is dominated by acicular tremolite within which is found uvarovite overgrowing fractured chromite (Fig. 23), and clots rich in Cr-diopside, plagioclase and uvarovite.

The granitic suite of rocks is characterized by an equigranular rock that contains quartz, plagioclase, K-feldspar and minor amounts of biotite, uncommonly muscovite, and sulphide.

In some granitic rocks a late-stage growth of stilpnomelane is observed. The more mafic assemblage contains up to 60% amphibole. The amphibole grains are xenomorphic and sharply zoned from blue-green cores to colorless rims.

## MINERALOGY AND MINERAL CHEMISTRY

All minerals discussed in this report were analysed on two different Camebax microprobes. A majority of the analyses were done on the microprobe in the Department of Earth and Atmospheric Sciences, Harvard University. This machine has three wavelength dispersive spectrometers and one energy dispersive spectrometer.

The analytical procedure was controlled by TASK, a software automation package developed at Sandia National Laboratories, which uses the Bence-Albee method for matrix corrections. A day's work would produce 100-150 spot analyses.

The second machine was the Camebax housed in the Department of Geological Sciences, McGill University. This machine has four automated wavelength dispersive spectrometers and is controlled by a Cameca software package that uses a ZAF correction procedure to handle matrix effects. On a good day 30-40 spot analyses were produced.

Both machines were used at 15 kv and 15 microamps sample current. The Harvard counting times varied from 10 to 40 seconds per element depending upon the counting statistics as monitored by the software control. The McGill machine was set to count for a fixed period of 20 seconds on each element. On both machines, well characterized minerals were used as standards. All analyses obtained for the twenty different rocks samples analyzed are presented in Appendix I. Selected analyses are also tabulated in the discussion below.

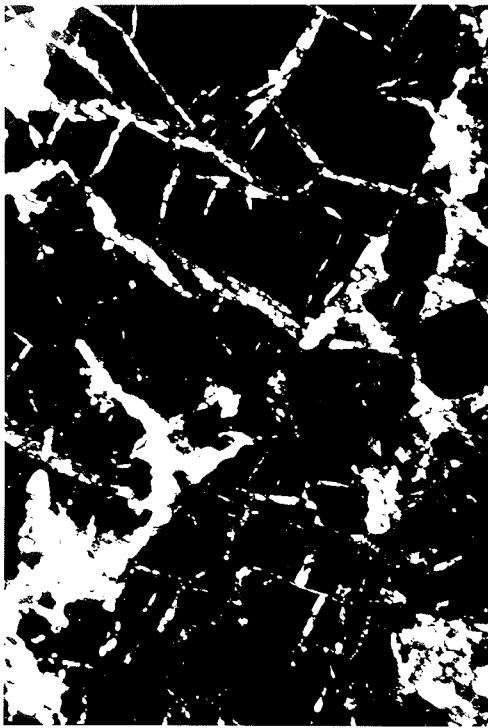


FIGURE 22 : Highly fractured chromite with darkening along fragment edges due to increased Fe/Mg and Cr/Al ratios (sample C-2-C, field of view is 3mm wide).



FIGURE 23 : Uvarovite growing within and around a fractured chromite grain (sample UVAROVITE, field of view is 3mm wide).



FIGURE 20 : Chromite layers in a serpentine matrix. This locality (Pit A) shows the graded nature of some of the chromite-rich layers.

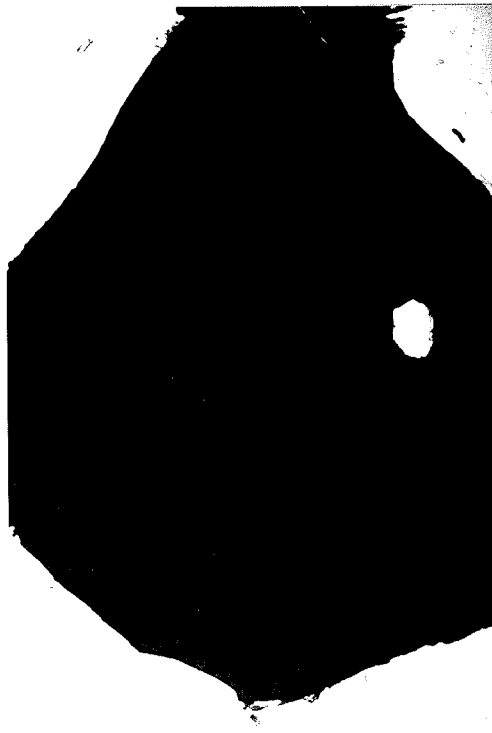


FIGURE 21 : A little-fractured chromite grain containing an olivine inclusion (sample STER-51, field of view is 3mm wide).

## Serpentine

Serpentine, by far the most common mineral in the ultramafic belt, displays little compositional variation. In all occurrences serpentine is interpreted to occupy the volume of precursor olivine or orthopyroxene. Although direct replacement of matrix olivine at Sterrett is not observed, serpentine after olivine is observed in chromite inclusions. Direct replacement of matrix olivine has been documented elsewhere in the Quebec ultramafic belt. Replacement of orthopyroxene was observed in several specimens where exsolved clinopyroxene lamellae remained in the pseudomorphed host. Microprobe analyses (Table 1) show that serpentine compositions do not vary greatly from the ideal composition  $\text{Mg}_3\text{Si}_2\text{O}_5(\text{OH})_4$ . Some iron replaces magnesium and minor solid solution, with entry of aluminum for silicon, towards clinocllore occurs. Several analyses contain NiO and are good indicators of an olivine precursor, as olivine does contain appreciable NiO (see below).

## Chromite

Because of the large solid solution field available in the spinel family of minerals (Fig. 24), chromite has a wide compositional variability (Table 2). Within any given sample there are generally two compositional subdivisions.

Chromite grains that are little fractured are quite homogeneous in composition except at their rims, where there is commonly an enrichment in iron (Fig. 25). In a number of samples, this is followed, by a ring of magnetite which is of the same composition as the dust-sized grains found in the serpentine matrix. Where fracturing of the chromite grains occurs there is a direct correlation between the intensity of fracturing and the depth of iron-enrichment into the grain or grain fragments. In several samples where the fracturing is extensive, the normally dark red-brown chromite becomes essentially opaque due to the near total substitution of  $\text{Fe}^{2+}$  for Mg and  $\text{Fe}^{3+}$  for Al. The iron within the chromite is mostly ferrous as seen on a Al-Cr- $\text{Fe}^{3+}$  plot (Fig. 26). The large chemical variability is found in the  $\text{Cr}/(\text{Cr} + \text{Al})$  and  $\text{Fe}/(\text{Fe} + \text{Mg})$  ratios (Fig. 27). In Fig. 27 the homogeneous central parts of chromite grains generally plot within a small area, and only toward the rim does the composition change towards higher  $\text{Cr}/(\text{Cr} + \text{Al})$  and  $\text{Fe}/(\text{Fe} + \text{Mg})$  ratios. Those chromite grains that are highly fractured show a more or less continuous trend on the  $\text{Cr}/(\text{Cr} + \text{Al}) - \text{Mg}/(\text{Fe} + \text{Mg})$  plot. Where chromite is a disseminated phase the compositional variation is similar to that shown by the highly fractured grains. This is to be expected in light of the fact that these grains are exposed to a much larger reservoir of iron than grains from massive chromite.

Based upon chemistry, Thayer (1960, 1970) has proposed that chromite from ultramafic layered intrusions can be discriminated from chromite found in Alpine-type ultramafic bodies. Furthermore, Evans and Frost (1975) have proposed that metamorphic chromites are also chemically distinct. A plot of representative chromite analyses from the Sterrett area onto the various fields (Fig. 27) proposed by Thayer (1960, 1970) and Evans and Frost (1975) indicates that the Sterrett chromites are not metamorphic, but are generally Alpine with significant overlap into the layered complex field.

One further point about chromite composition needs mention as it bears on the petrogenesis of these rocks. Chromites from the chromite-rich lenses in dunites have compositions that are similar to the disseminated chromite found in the peridotites surrounding the chromite-rich lenses. This compositional similarity suggests that all these rocks crystallized from spatially and temporally related magmas having homogeneous compositions. This is in sharp contrast to other localities, Mont Albert for example (Trzcienski, unpublished data), where massive chromite has a

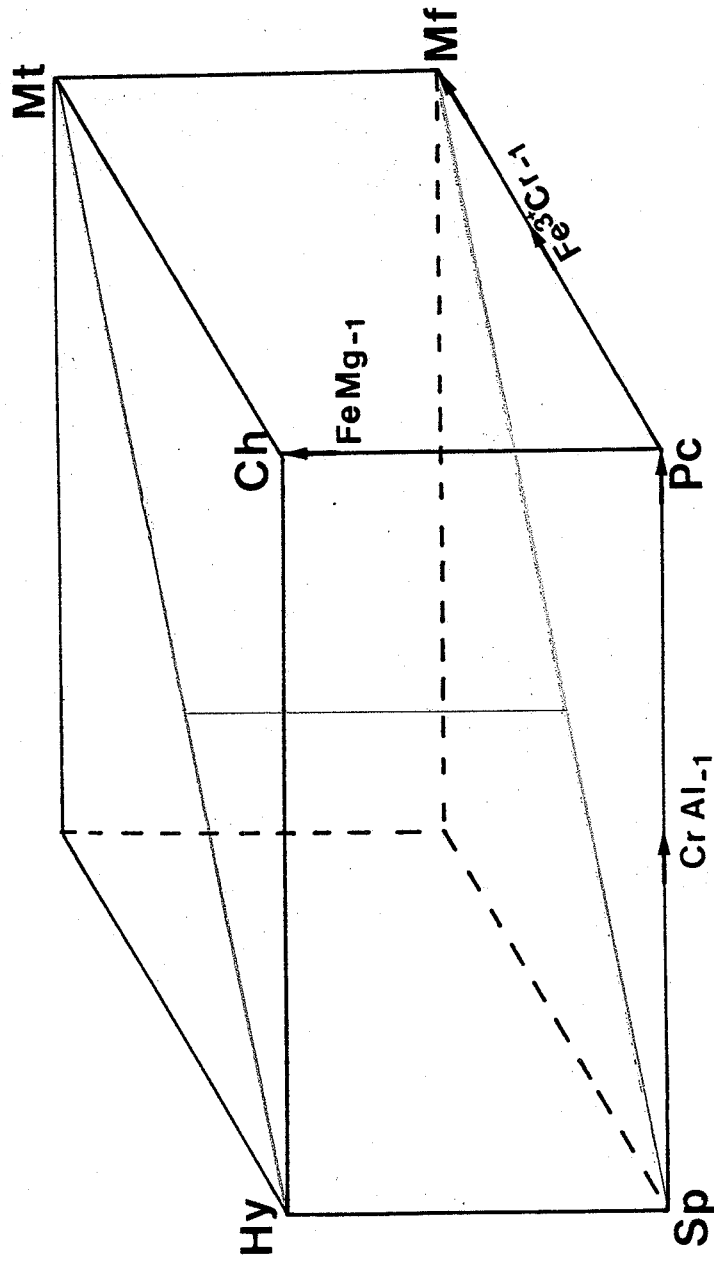


Figure 24: The compositional relationships found amongst the various spinel(Sp) family minerals hercynite(Hy), picrochromite(Pc), chromite(Ch), magferrite(Mf), and magnetite(Mt) and their cation substitutions.

Table 1 Representative serpentine analyses

	CR-PIT-2-4B	CR-PIT-2-13	STER-4D	STER-6B	STER-1A
SiO <sub>2</sub>	42.88	42.92	44.11	43.03	42.00
TiO <sub>2</sub>	.00	.00	.04	.00	.00
Al <sub>2</sub> O <sub>3</sub>	3.39	.74	.50	.05	2.27
Cr <sub>2</sub> O <sub>3</sub>	1.50	.14	.32	.07	.00
FeO	3.68	4.06	2.20	1.71	2.35
MnO	.04	.07	.00	.03	.00
NiO	.12	.16	.00	.11	.00
MgO	38.25	37.64	39.37	39.18	40.38
CaO	.01	.00	.05	.00	.00
Na <sub>2</sub> O	.00	.00	.00	.00	.00
K <sub>2</sub> O	.00	.00	.00	.00	.00
Total	89.87	85.73	86.59	84.18	87.00

Table 2 Representative chromite analyses

	STER-6B-1	STER-6B-4	STER-4D-9	CR-PIT-2-4	CR-PIT-2-5	CR-PIT-2-9	C-2-D-3
SiO <sub>2</sub>	.04	.06	.03	.04	.15	.11	.04
TiO <sub>2</sub>	.22	.21	.08	.03	.55	.15	.03
Al <sub>2</sub> O <sub>3</sub>	16.21	14.91	14.99	17.66	.34	4.06	22.91
Fe <sub>2</sub> O <sub>3</sub> †	3.71	5.51	3.15	2.91	18.47	6.20	4.44
Cr <sub>2</sub> O <sub>3</sub>	52.06	49.88	57.02	51.38	47.76	60.26	46.62
V <sub>2</sub> O <sub>3</sub>	.11	.11	.00	.05	.16	.13	.00
FeO	14.91	15.57	13.73	16.48	29.76	25.90	8.83
MnO	.15	.18	.50	.16	1.72	.71	.31
NiO	.13	.12	.00	.01	.08	.07	.21
MgO	12.92	11.92	13.74	11.97	.29	4.44	17.39
CaO	.02	.01	.00	.18	.34	.09	.00
Total	100.48	98.48	103.24	100.87	99.62	102.12	100.78

	C-2-D-8B	STER-GT-1B-1	STER-GT-1B-9	PIT-G-1	PIT-G-1-14	UVAROVITE-34
SiO <sub>2</sub>	.01	.08	.04	.09	.13	.07
TiO <sub>2</sub>	.02	.48	.41	.25	.17	.03
Al <sub>2</sub> O <sub>3</sub>	3.16	19.43	13.69	13.64	23.53	21.54
Fe <sub>2</sub> O <sub>3</sub> †	4.90	5.97	5.06	3.66	4.30	3.53
Cr <sub>2</sub> O <sub>3</sub>	63.47	46.13	52.91	55.72	46.06	46.65
V <sub>2</sub> O <sub>3</sub>	.00	.56	.47	.16	.15	.00
FeO	19.95	14.51	16.69	15.03	13.51	14.43
MnO	.94	.17	.17	.41	.21	.14
NiO	.06	.16	.14	.21	.11	.09
MgO	7.59	13.82	11.76	12.56	14.86	13.45
CaO	.00	.00	.00	.05	.00	.32
Total	100.10	101.31	101.34	101.78	103.03	100.25

Fe<sup>3+</sup> calculated from stoichiometry



FIGURE 25 : Slightly fractured chromite with an iron  
-enriched halo surrounding a homogeneous core  
(sample STER-6B, field of view is 3mm wide).



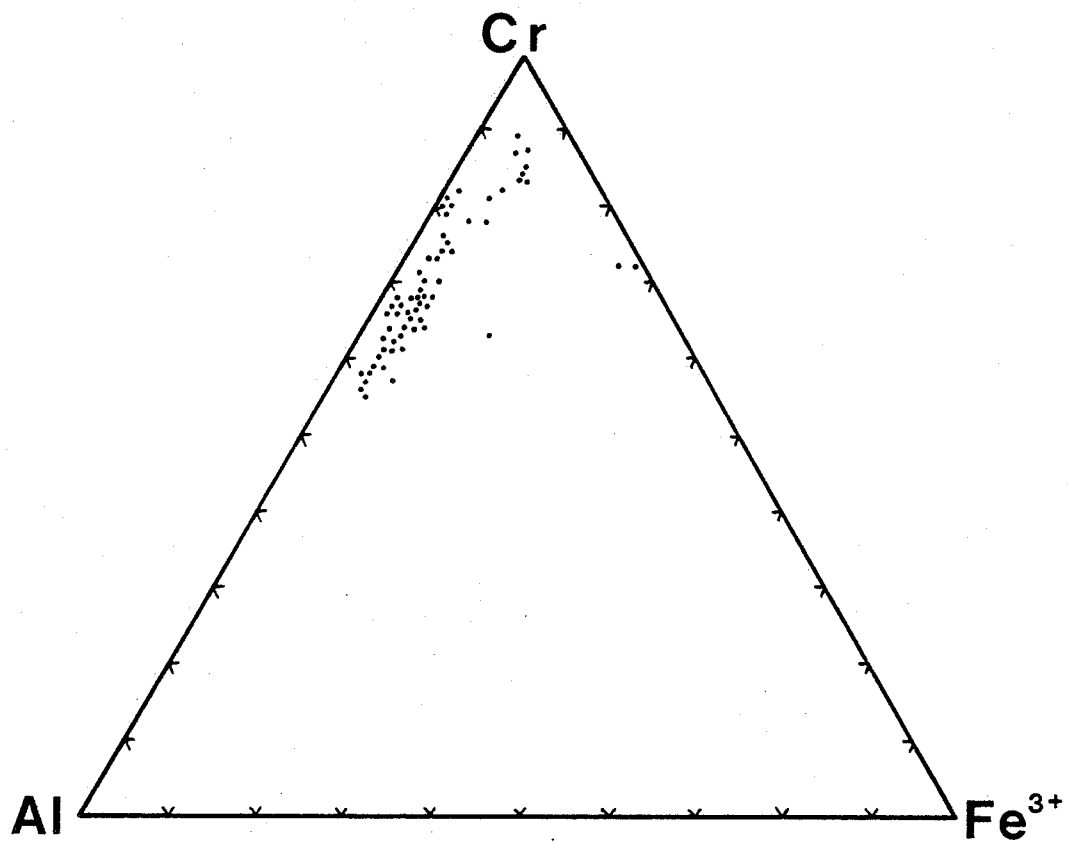


Figure 26: Plot of Al-Cr-Fe<sup>3+</sup> distribution in Sterrett chromites. Many points represent multiple analyses.

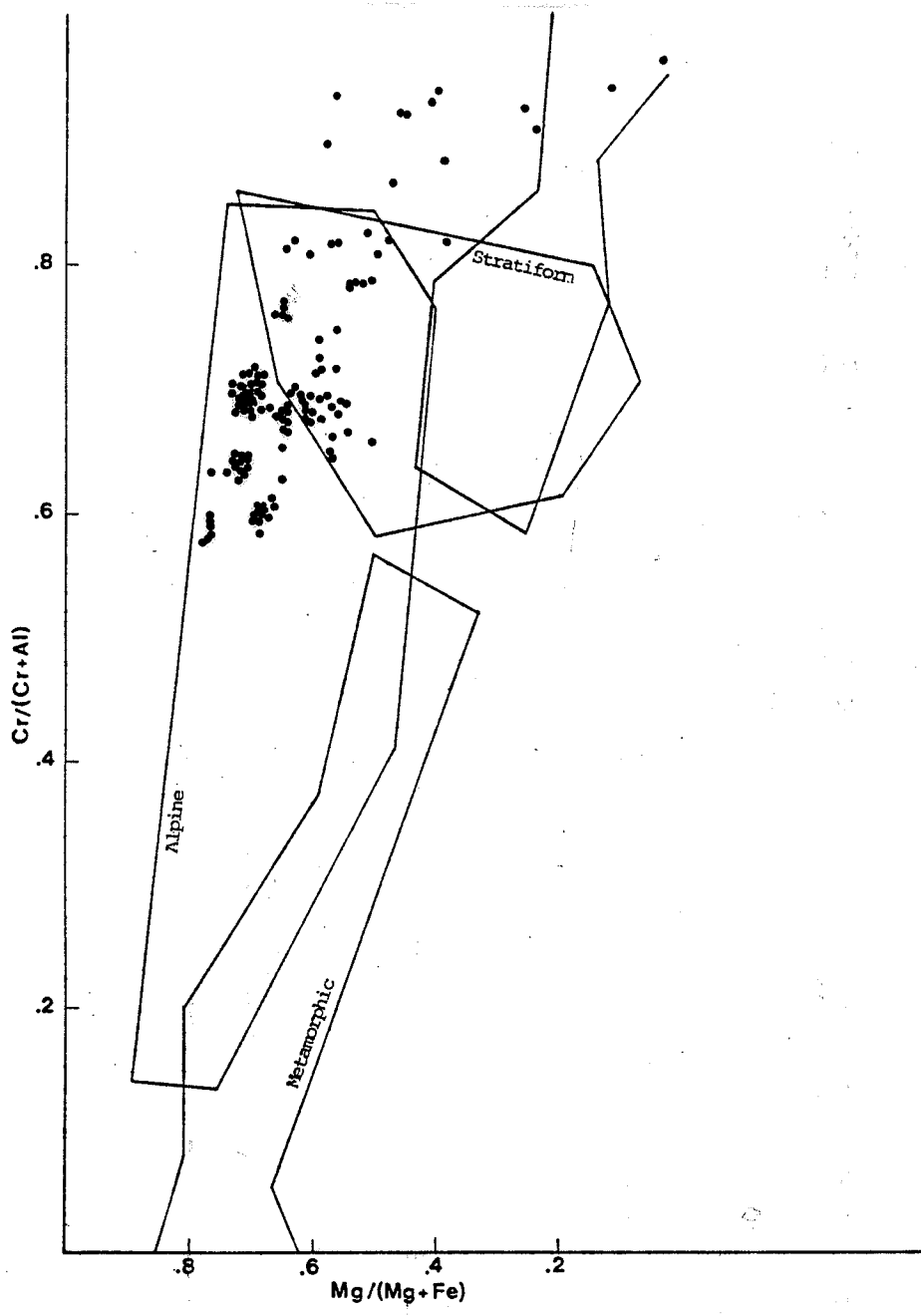


FIGURE 27 :  $\text{Cr}/(\text{Cr} + \text{Al})$  vs  $\text{Mg}/(\text{Mg} + \text{Fe})$  plot of Sterrett chromites used for discriminating Alpine from stratiform from purely metamorphic chromites.

composition quite different from that of the chrome spinel that is found in the rock hosting the chromite lenses.

### **Chlorite**

Chlorite occurs most commonly as isolated sheaves of crystals enclosed by serpentine, and along fracture zones or around chromite grains. It is easy to recognize and distinguish from serpentine by its light-grey birefringence and slight rotary extinction.

The compositions (Table 3) determined by microprobe indicate a large compositional variability between samples as well as between grains within a sample. All the chlorites are highly magnesian ( $\text{MgO} > 25.00\%$ ) but the Al/Si ratios change rather drastically and in some, the iron content is quite high. There may actually be two different chlorite-like phases present as characterized by analyses from sample Pit-G-1 (49 & 50) which come from intermingled grains. The contribution of chromite to chlorite growth is quite evident where the matrix is serpentine. Thin rims of chlorite around chromite grains probably formed by reaction of serpentine with aluminum from the chromite.

### **Olivine**

Olivine in the Sterrett mine area is found only as small inclusions within chromite.

Olivine is optically recognizable from chromite between X-nicols by its moderate birefringence. In several occurrences the olivine is incipiently altered to serpentine, further supporting the argument for serpentine resulting from olivine alteration in the matrix of the chromitites. Compositionally (Table 4) the olivine is fosterite ( $\text{Mg}/(\text{Mg} + \text{Fe}) > 0.90$ ). There is essentially no zoning within individual grains, and all analyses show a significant nickel content (0.50-1.00% NiO).

Variation from sample to sample is slight as is variation with olivine (sample RB-2, Table 4) from the Reed-Belanger deposit south of Thetford Mines.

### **Magnetite**

Within the serpentinites, magnetite is most commonly a by-product of the serpentinitization process. It forms either as concentrations of minute particles along serpentine grain boundaries or as rims on chromite. Where it is separated from chromite it is nearly pure  $\text{Fe}_3\text{O}_4$  (samples: STER-1A, STER-6A, STER-6B, Table 5) but where it is part of the alteration of chromite (STER-1B, Table 5) the  $\text{Cr}_2\text{O}_3/\text{Fe}_2\text{O}_3$  variability is significant. No magnetite of arguably magmatic origin was observed anywhere in the Sterrett Mine area.

### **Sulphides**

Although not common in the chromitites, Fe-Ni or Ni-sulphides do occur in the ultramafic rocks in the Sterrett mine area. Heazlewoodite (Table 6) is the most often identified sulphide, and is found in rocks where disseminated chromite occurs. One sample of chromitite (CR-PIT-2, Table 6) contained pentlandite.

Table 3 Representative analyses of chlorite

	CR-PIT-2-8B	STER-1A-8	C-2-D-39B	STER-GT-1B	STER-GT-1B	PIT-6-1-48	PIT-6-1-49	PIT-6-1-50
				-112	-114			
SiO2	32.62	35.34	33.03	26.90	31.44	39.22	35.28	27.02
TiO2	.02	.00	.00	.00	.00	.02	.00	.00
Al2O3	14.41	13.60	13.80	21.68	16.64	13.62	9.86	21.11
Cr2O3	2.70	.00	3.03	.00	.00	.01	.00	.02
FeO	.80	6.82	4.98	7.73	2.26	5.74	1.71	11.89
MnO	.00	.07	.21	1.12	.06	.43	.05	1.29
NiO	.08	.07	.57	.00	.00	.00	.00	.00
MgO	34.78	.00	30.99	26.14	33.82	25.44	37.01	24.64
CaO	.03	33.26	.03	.03	.02	.00	.00	.00
Na2O	.00	.00	.00	.02	.00	.00	.00	.00
K2O	.00	.00	.00	.02	.01	4.69	.00	.03
Total	85.44	89.16	86.64	83.64	84.25	89.17	83.91	86.00

Table 4 Representative analyses of olivine

	STER-GT-2A-	STER-GT-2A-	PIT-6-1-	STER-GT-3C-	STER-51-	C-2-C-	STER-4D-	RB-2-
SiO2	41.09	40.73	40.85	40.82	41.41	40.86	42.71	41.33
Cr2O3	.09	.29	.44	.22	.72	.64	.59	.70
FeO	5.36	4.89	4.26	3.35	3.60	3.44	3.85	3.05
MnO	.10	.08	.06	.05	.05	.07	.08	.04
NiO	1.02	1.05	.97	.53	.65	.69	.00	.64
MgO	52.79	52.94	53.74	54.07	55.03	54.54	54.02	53.75
CaO	.06	.01	.02	.02	.02	.00	.02	.04
Total	100.51	99.99	100.34	99.06	101.48	100.24	101.27	99.55

Table 5 Representative analyses of magnetite

	STER-1A-6	STER-6B-11	STER-1B-2	STER-1B-12	STER-6A-2
SiO <sub>2</sub>	1.25	.08	2.66	1.01	.13
TiO <sub>2</sub>	.67	.08	.00	.00	.06
Al <sub>2</sub> O <sub>3</sub>	.10	.00	.01	.02	.03
Fe <sub>2</sub> O <sub>3</sub> †	66.02	67.68	68.58	64.32	66.98
Cr <sub>2</sub> O <sub>3</sub>	.06	.25	1.00	1.60	.14
FeO	30.02	30.03	23.96	28.91	29.60
MnO	.54	.00	.22	.23	.00
NiO	.08	.35	.87	.76	.42
HgO	1.88	.30	3.11	1.26	.36
Total	100.62	98.77	100.41	98.11	97.72

Table 6 Representative analyses of sulphides

	CR-PIT-2-1	CR-PIT-2-2	CR-PIT-2 -10B	STER-6A-2	STER-1A-4	STER-1B-1	STER-1B-6
S	33.00	34.41	33.11	26.92	26.86	27.12	27.01
Ni	38.48	38.37	38.36	73.27	72.73	72.88	72.47
Fe	27.72	27.93	27.78	.18	.25	.10	.14
Cu	.00	.05	.00	.00	.00	.00	.00
Zn	.03	.00	.00	.00	.00	.00	.00
Total	99.23	100.76	99.25	100.37	99.84	100.10	99.62

## Clinopyroxene

Diopside is found both as inclusions within chromite and as xenomorphic crystals in several different types of occurrence. Cr-diopside (Table 7, STER-6B, STER-3C), found as inclusions in chromite, is iron-poor and represents a re-equilibrated (with chromite), early igneous crystallate.

Late, chrome-poor diopside has been found in one chromitite sample associated with an anorthosite layer. This diopside (Table 7, STER-GT-1B) is more aluminous, sodic and iron-rich than the early, entrapped diopside.

The third type of diopside is found in clots in meta-anorthosite. This diopside is characterized by a moderately high Na-content that distinguishes it chemically from the two types of diopside interpreted to be igneous in origin.

## Amphibole

Amphibole is similar to diopside in its occurrence, and is found both as an inclusion in chromite and as tabular to acicular crystals in meta-anorthosite. The major, and easily recognizable, chemical difference between the two types of occurrences is that the amphibole inclusions are much more aluminous and chrome-rich than the matrix amphibole (Table 8). Whether this is an igneous amphibole or a product of a diopside plus chromite re-equilibration is at this time unknown. One analyzed sample from the Reed-Belanger deposit at Cariboo Lake near Thetford Mines, has amphibole and diopside inclusions in the same chromite grain. In contrast the metamorphically formed amphibole is more iron-rich than that found as chromite inclusions and also contains some sodium.

In the felsic rocks where amphibole is present, the grains of amphibole are commonly zoned from a bluish core to a colorless rim (Fig. 28). The compositional variation is from sodium-rich cores to sodium-poor rims (Table 8).

## Mn-Ilmenite-Pyrophanite

Mn-ilmenite-pyrophanite grains, initially thought to be small chromite grains because of their deep red to near opaque optical properties, have been identified in two samples. Compositionally, the two minerals, ilmenite and pyrophanite form a solid solution series between  $\text{FeTiO}_3$  and  $\text{MnTiO}_3$ . One set of analyses (STER-1A, Table 9) comes from a late-stage differentiated pyroxenite dike that crosscuts the ultramafic sequence. The other sample (STER-GT-2A, Table 9) is from chromitite associated with an anorthositic layer. The differentiated dike rock contains compositions nearer the ideal pyrophanite composition although there remains significant iron. Both occurrences contain significant  $\text{MgO}$  and  $\text{V}_2\text{O}_3$ . The dike rock also contains magnetite intergrown with the pyrophanite.

## Garnet

Two varieties of garnet have been recognized in rocks that are interpreted to be anorthositic in origin. Where it is associated with or directly overgrows chromite (Fig. 23), the garnet is grossular-uvarovite (Table 10). Where garnet grows as minute "cauliflower-like" grains in meta-anorthosite (Fig. 29), it is grossular-spessartine (Table 10). Both garnet types show a wide variation in the grossular-uvarovite and grossular-spessartine ratios. The other two major garnet components almandine ( $\text{FeO}$ ) and pyrope ( $\text{MgO}$ ) are of minor importance.

Table 7 Representative analyses of clinopyroxene

	STER-6B-13	STER-3C-3	UVAROVITE-5	UVAROVITE-8	UVAROVITE-24	STER-6T-1B	STER-6T-1B
						-117	-119
SiO2	53.97	54.05	53.92	54.32	54.21	52.41	53.54
TiO2	.00	.07	.06	.02	.00	.21	.10
Al2O3	.10	.97	2.04	1.97	.43	2.09	1.07
Cr2O3	1.63	.91	2.05	1.24	2.91	.13	.05
FeO	.47	1.07	4.66	4.37	5.19	6.80	6.64
MnO	.00	.03	.19	.20	.26	.21	.22
NiO	.00	.05	.00	.00	.00	.00	.00
MgO	17.48	17.90	12.70	13.44	13.47	14.81	15.73
CaO	24.90	25.22	21.74	22.55	22.99	21.08	23.33
Na2O	.00	.00	1.81	1.62	1.19	.21	.15
Total	98.55	100.27	99.17	99.73	100.65	97.95	100.83

Table 8 Representative analyses of amphibole

	PIT-6-1-4	PIT-6-1-45	PIT-6-1-46	UVAROVITE	UVAROVITE	UVAROVITE	UVAROVITE	RB-2-4	RB-2-7	CODD-2-13	CODD-2-28
				-13	-17	-20					
SiO2	46.67	55.81	54.06	57.32	57.37	55.58	44.75	44.07	54.07	54.07	48.10
TiO2	.50	.03	.03	.00	.00	.01	.48	.48	.08	.08	.78
Al2O3	8.77	.76	2.59	.18	.43	.35	10.16	10.40	1.12	1.12	6.36
Cr2O3	3.11	.03	.03	.07	.00	.59	3.84	3.85	.14	.14	.00
FeO	2.03	3.86	3.94	4.36	4.56	10.41	1.56	1.63	21.40	21.40	15.79
MnO	.08	.66	2.03	.13	.11	.51	.05	.02	.84	.84	.26
NiO	.24	.00	.00	.00	.00	.00	.15	.14	.00	.00	.00
MgO	19.56	21.55	19.44	20.97	21.20	16.86	19.59	19.59	11.75	11.75	12.71
CaO	11.75	12.52	12.97	13.19	13.27	12.68	12.71	12.81	3.97	3.97	11.63
Na2O	.00	.07	.40	.04	.10	.09	.00	.00	.00	.00	1.66
K2O	.00	.13	.30	.02	.03	.04	.00	.00	.09	.09	.21
Total	92.71	95.42	95.79	96.28	97.07	97.12	93.29	92.99	97.86	97.86	97.50

Table 9 Representative analyses of Mn-ilmenite and pyrophanite

	STER-1A-1	STER-1A-2	STER-GT-2A -15	STER-GT-2A -16
SiO2	1.28	.25	.48	.62
TiO2	52.49	53.18	51.66	52.14
Al2O3	.27	.00	.32	.25
V2O5	.32	.37	.32	.33
FeO	11.86	11.20	28.15	28.19
MnO	32.03	33.90	17.27	15.77
NiO	.02	.04	.04	.04
MgO	2.63	1.33	1.70	1.17
CaO	.01	.02	.04	.05
Total	100.91	100.29	99.98	98.56

Table 10 Representative analyses of garnet

	UVAROVITE -3	UVAROVITE -10	UVAROVITE -12	STER-GT-1B -11	STER-GT-1B -12	STER-GT-1B -18	STER-GT-1B -21	PIT-6-1-20	PIT-6-1-23	PIT-6-1-33
SiO2	37.55	38.30	38.47	38.84	38.81	39.27	39.52	38.49	38.71	38.54
TiO2	.36	.18	.18	.00	.00	.00	.00	.00	.00	.00
Al2O3	10.98	14.24	13.74	21.48	21.75	21.79	21.88	22.78	22.40	22.65
CR2O3	13.06	9.17	9.65	.02	.00	.02	.01	.00	.00	.00
FeO	2.34	2.56	2.39	.97	1.29	1.29	.95	1.91	1.62	1.75
MnO	.39	.58	.57	13.67	9.25	7.96	4.72	10.19	6.85	4.78
MgO	.00	.02	.03	.14	.63	.05	.04	.06	.09	.05
CaO	34.73	35.28	34.98	24.73	27.30	29.31	32.55	26.66	30.35	32.30
Total	99.41	100.33	100.01	99.85	99.03	99.69	99.67	100.09	100.02	100.07



## Feldspar

Feldspars have been found only in the granitic rocks and the anorthositic layers associated with the chromitites. K-feldspar in the uvarovite-amphibole anorthositic rock occurs as minute grains (5-10 m) and contains a moderate amount of barium (Table 11). K-feldspar in association with the grossular-rich anorthositic layers is found only as a rim/vein filling in plagioclase. This K-feldspar is barium-rich (Table 11) with up to one-quarter of the K-site filled by the celsian component. Plagioclase varies from nearly pure albite in the uvarovite-amphibole rock (Table 11) to zoned crystals with variable anorthite (Table 11) content in the grossular-rich layers. In the granitic rocks, K-feldspar is close to the ideal K-feldspar composition while plagioclase is mostly albite (Table 11).

Several of these rocks called "granite" consist almost totally of albite-quartz.

## Calc-silicate minerals

Within the anorthositic layers, pumpellyite, prehnite and zoisite are also found.

Prehnite is nearly of the end member composition  $\text{Ca}_2\text{Al}_2\text{Si}_3\text{O}_{10}(\text{OH})_2$  (Table 12) with trace amounts of iron, manganese and potassium. It is commonly found replacing plagioclase in the matrix of the white anorthositic layers sandwiched between chromitite layers (Fig. 29).

Pumpellyite, initially identified by EDS analysis on the microprobe, occurs within the prehnite-plagioclase matrix as small (<40 micron) needle-like grains. Compositionally it is near the Mg-Al-pumpellyite composition  $\text{Ca}_4\text{MgAl}_5\text{Si}_6\text{O}_{21}(\text{OH})_7$  (Table 12) (Schiffman and Liou, 1980) which is more aluminous than normal pumpellyite ( $\text{Ca}_4\text{Mg}_2\text{Al}_4\text{Si}_6\text{O}_{21}(\text{OH})_7$ ). Minor amounts of MnO and FeO substitute for MgO.

Zoisite is readily identifiable by its tabular shape, low birefringence and its orthorhombic, length-fast optical properties. Some zoning occurs mainly via the Al-Fe exchange (Table 12). This iron substitution appears to be totally accommodated within the zoisite structure as there is no optical evidence of a moderately birefringent monoclinic phase (epidote).

## GEOCHEMISTRY

Eighteen samples representing the range of rock types were submitted for normal whole rock major element and trace element analyses. In addition several of these samples were selected for Pd, Pt and Au analysis and rare-earth element analyses. Major and trace element analyses were carried out by the geochemical laboratories in the Dept. of Geological Sciences at McGill University, Montreal. Pt, Pd, Au determinations at the PPB level were done by X-RAY ANALYSIS LABORATORIES of Toronto and the rare-earth elements were done in the geochemical laboratory at Dept. de la Géologie, Université de Montréal. All of the samples are either highly serpentized or now contain minerals that have been produced by metamorphism. The high degree of hydration implied by the serpentization process puts severe constraints on the validity of recalculating anhydrous original bulk compositions. In spite of this problem some differences are noted (Table 13) and CIPW norms (Appendix II) have been calculated for the analyses on an anhydrous basis.

Several inferences can be drawn from this exercise but one must use caution. With respect to the major elements, the "mackerel-striped" rock that commonly lies adjacent to chromitite (sample STER-FG-4, Table 13) is not much different from the

Table 11 Representative analyses of feldspars

	UVAROVITE -29	UVAROVITE -27	PIT-6-1-52	PIT-6-1-54	PIT-6-1-55	PIT-6-1-57	CODD-2-5	CODD-2-34
SiO2	68.46	62.07	54.44	55.69	60.71	59.43	68.42	61.96
Al2O3	19.66	17.00	21.43	20.82	23.78	25.09	19.87	20.54
FeO	.05	.67	.20	.10	.05	.14	.00	.46
CaO	.27	1.61	.04	.04	4.01	6.31	.05	.03
BaO	.03	2.16	12.82	11.16	.07	.03	.00	.00
Na2O	11.49	.20	.45	.44	8.77	7.98	11.93	.31
K2O	.16	13.51	11.43	10.37	.57	.04	.03	15.84
Total	100.12	97.22	100.81	98.62	97.96	99.02	100.30	99.14

Table 12 Representative analyses of prehnite(PR), pumpellyite(PU) and zoisite(ZO).

	STER-6T-1B -105(PR)	STER-6T-1B -14(PU)	STER-6T-1B -16(PU)	STER-6T-1B -29(ZO)	STER-6T-1B -101(ZO)	PIT-6-1 -43(PR)	PIT-6-1 -64(PR)	PIT-6-1 -35(ZO)	PIT-6-1 -38(ZO)
SiO2	41.47	38.41	37.49	38.90	39.06	42.00	42.34	38.67	38.62
Al2O3	23.86	26.27	26.20	31.96	33.22	24.38	24.32	30.95	33.63
FeO	.04	.68	.69	1.21	.21	.16	.07	3.29	.15
MnO	.03	.40	.58	.00	.96	.00	.10	.11	.00
MgO	.00	3.29	3.75	.00	.06	.00	.01	.06	.05
CaO	25.83	23.22	22.53	23.89	23.73	26.55	26.46	23.55	22.73
K2O	.15	.00	.00	.01	.00	.07	.07	.00	.00
Total	91.38	92.27	91.24	95.97	97.24	93.16	93.37	96.63	95.18

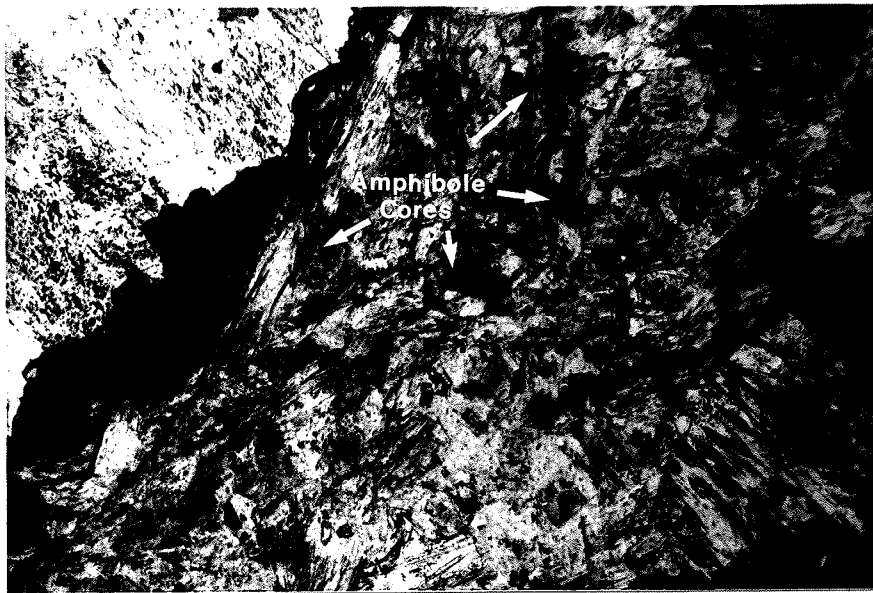


FIGURE 28 : Amphiboles with dark cores and colorless rims in a "granitic" rock associated with the ultramafic rocks (field of view is 3mm wide).

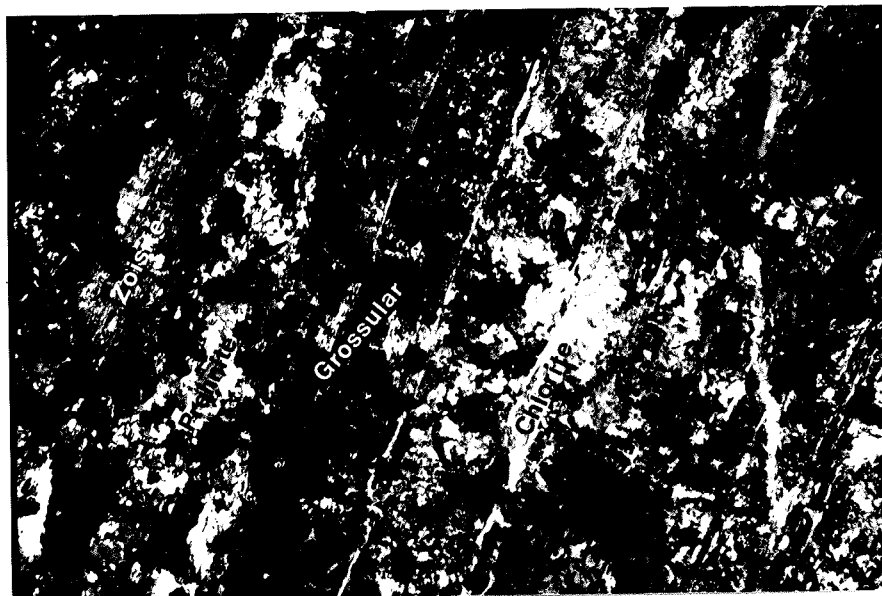


FIGURE 29 : Prehnite, zoisite (to the left of the photo), grossular (black), and chlorite (to the right of the photo) from a meta-anorthosite layer. Pumpellyite is too fine grained to be seen. The parallel, slightly inclined fractures are perpendicular to the chromite-anorthosite contact (sample STER-GT-1B, field of view is 3mm).

Table 13: Whole rock analyses of rocks from the Sterrett mine area

	STER-GT-1Q	STER-GT-1B	STER-GT-1Z	UVAROVITE	STER-G-3B	STER-FG-1	STER-FG-2	STER-FG-4
SiO2	36.06	36.10		55.98	65.47	37.92	38.43	37.32
TiO2	.14	.03		.08	.11	.01	.13	.03
Al2O3	11.60	28.23		1.57	17.73	.44	.40	.78
Fe2O3	8.66	3.10		7.95	1.33	8.76	8.01	8.53
MnO	.26	.54		.20	.04	.07	.06	.07
MgO	29.73	16.42		17.43	2.42	38.38	37.40	36.76
CaO	3.23	3.88		13.77	1.83	.29	.85	1.69
Na2O	.01	.01		.21	8.68	.01	.01	.01
K2O	.04	3.06		.13	1.51	.01	.01	.02
P2O5	.01	.02		.04	.04	.01	.02	.02
L.O.I	10.73	8.92		1.63	.60	14.20	13.85	14.21
TOTAL	100.47	100.31		98.99	99.76	100.10	99.17	99.44
V	204.00	10.00		20.00	10.00	21.00	17.00	35.00
Cr2O3	2997.00	138.00		4866.00	56.00	3320.00	4363.00	5519.00
Ni	212.00	63.00		2605.00	48.00	2431.00	2643.00	2710.00
BaO	10.00	1254.00		11.00	936.00	10.00	22.00	10.00
Nb	8.00	7.00	5.00	9.00	15.00	8.00	8.00	8.00
Zr	40.00	44.00	38.00	39.00	83.00	38.00	38.00	39.00
Y	5.00	5.00	5.00	10.00	28.00	5.00	5.00	5.00
Sr	18.00	139.00	16.00	26.00	87.00	21.00	22.00	37.00
Rb	5.00	56.00	5.00	5.00	8.00	5.00	5.00	5.00
Pb	5.00	5.00	5.00	5.00	5.00	5.00	5.00	5.00
Th	5.00	5.00	5.00	5.00	5.00	5.00	5.00	5.00
U	9.00	8.00	13.00	10.00	10.00	9.00	11.00	12.00
Ga	5.00	9.00	12.00	5.00	16.00	5.00	5.00	5.00
LA		2.30				.10	.21	1.00
CE		1.90				1.50	1.50	ND
ND		.70				ND	.60	ND
SM		ND				ND	.01	ND
EU		.46				.03	.02	.03
TB		ND				.06	ND	.06
HO		.09				ND	ND	ND
TM		ND				ND	ND	ND
YB		ND				ND	ND	ND
LU		ND				ND	ND	ND
Pt (PPB)	10.00		10.00		<10.00	10.00	10.00	<10.00
Pd (PPB)	9.00		2.00		2.00	3.00	6.00	<2.00
Au (PPB)	4.00		17.00		<1.00	<1.00	<1.00	<1.00

Table 13 (CONTINUED): Whole rock analyses of rocks from the Sterrett mine area

	STER-1A	STER-1B	PIT-8	CODD-21A	CODD 0+508	CODD 2+45	STER-300	STER-48	STER-49	STER-44
SiO2	33.88	35.07		78.27	60.82	70.30	19.78	41.56		75.36
TiO2	.13	.01		.08	.24	.17	.01	.01		.11
Al2O3	13.05	.54		12.90	14.43	13.84	.74	.64		13.56
Fe2O3	3.37	5.78		.64	6.82	3.91	5.12	7.16		1.12
MnO	.21	.08		.02	.12	.09	.45	.07		.04
MgO	36.32	42.07		.07	4.83	1.69	28.06	37.20		.52
CaO	.01	.10		.36	4.61	2.11	15.69	.12		.82
Na2O	.01	.01		6.93	6.73	6.24	.01	.01		5.71
K2O	.01	.04		.17	.59	.75	.01	.01		1.99
P2O5	.01	.01		.07	.06	.06	.01	.01		.08
L.O.I	13.39	15.58		.42	.54	.55	29.80	11.70		.48
TOTAL	100.39	99.29		99.93	99.79	99.71	99.68	98.49		99.79
V	10.00	14.00		10.00	131.00	56.00	34.00	28.00		10.00
Cr2O3	19.00	41.13		15.00	312.00	41.00	7856.00	42.12		17.00
Ni	107.00	5143.00		10.00	116.00	31.00	982.00	2341.00		10.00
BaO	12.00	10.00		67.00	449.00	528.00	10.00	10.00		958.00
Nb	14.00	9.00	6.00	7.00	9.00	11.00	7.00	9.00	5.00	12.00
Zr	122.00	39.00	37.00	59.00	75.00	80.00	41.00	39.00	37.00	47.00
Y	6.00	5.00	5.00	10.00	7.00	8.00	5.00	5.00	5.00	15.00
Sr	16.00	21.00	16.00	58.00	156.00	238.00	249.00	18.00	33.00	115.00
Rb	5.00	5.00	5.00	5.00	6.00	8.00	5.00	5.00	5.00	26.00
Pb	5.00	5.00	5.00	5.00	5.00	5.00	5.00	5.00	7.00	6.00
Th	5.00	5.00	5.00	5.00	5.00	5.00	5.00	5.00	9.00	5.00
U	125.00	9.00	10.00	9.00	11.00	10.00	13.00	13.00	11.00	9.00
Ga	5.00	5.00	6.00	12.00	14.00	9.00	5.00	5.00	16.00	11.00
LA	.60	.20		5.10	3.00			.25		5.80
CE	1.90	4.40		9.00	5.00			1.00		12.00
ND	.80	ND		3.50	1.90			.40		4.90
SM	.34	.01		.79	.67			.01		1.87
EU	.01	.03		.08	.25			.06		.64
TB	.20	.05		.18	ND			.09		.42
HD	.39	ND		.30	ND			.18		ND
TM	.10	.03		ND	ND			ND		ND
YB	1.14	ND		1.20	.80			.02		1.70
LU	.23	ND		.18	.17			ND		.24
Pt (PPB)		10.00	30.00						10.00	
Pd (PPB)		3.00	5.00						<2.00	
Au (PPB)		<1.00	<1.00						<1.00	

coarse or the finer grained peridotite (STER-FG-1,2). The "mackerel-striped" rocks, however, have lower normative orthopyroxene, more normative clinopyroxene, and comparable normative olivine (Appendix II). Significantly higher Cr + Ni in rocks inferred to be dunitic and associated with chromitite is probably a better discriminant (see sample STER-1B, Table 13) than calculated norms. The late stage cross-cutting pyroxenite dikes are characterized by high aluminum content and a depletion of Cr + Ni (STER-1A, Table 13). Mineralogically the latter is reflected in the high percentage of chlorite, rather than a serpentine mineral, in the dike rock. Chlorite, rather than serpentine, in material representing the reaction zone between chromitite and anorthosite is also reflected in the high Al<sub>2</sub>O<sub>3</sub> content of the analysis (STER-GT-1Q, Table 13). Three analyses of chromitite (STER-GT-1Z, PIT-B, STER-49, Table 13) proved fruitless as the analytical procedure was not capable of handling analyses where Cr<sub>2</sub>O<sub>3</sub> exceeded 35 weight percent. The one analysis (STER-GT-1B, Table 13) of material from an "anorthosite" band reflects the high aluminum expected for a feldspar-rich rock. The high magnesium reflects the surrounding and intergrown chlorite. This chlorite is derived either from an original Mg-rich igneous mineral in the anorthosite band or chlorite produced by reaction between the anorthosite band and the surrounding ultramafic layers.

Compared to the ultramafic rocks, the felsic rocks in the Sterrett area have widely varying SiO<sub>2</sub> compositions (55 to 75 weight %, Table 13) and a higher concentration of alkali metals or their substitutes (Ba, Rb, Sr).

Of the ten samples submitted for Pd, Pt and Au analyses all but one showed background levels for Pt. The one exception (Sample PIT-B, Table 13) is one of few to contain pentlandite rather than heazlewoodite. Au appeared above background in only the samples (STER-GT-1Z, 1Q, Table 13) associated with an anorthositic band. Pd, as the other two elements, was only slightly above background.

## PETROGENESIS

Because of the highly altered nature of the rocks in the Sterrett Mine area, a determination of the original rock types is somewhat speculative. In spite of this alteration, comparison of mineralogies, chemistries and field relations in the Sterrett area to other, similar, less altered sequences elsewhere in the world allows the drawing of certain conclusions about the geologic evolution of these rocks. This comparison indicates that the Sterrett area rocks have come from an igneous parentage that has subsequently undergone various degrees of metamorphism.

### Igneous History

Mineralogically, chromite is the major remnant igneous phase. Olivine and clinopyroxenes within some of these chromites are also igneous in origin. The linear trend of the chromite-rich band in the field, fine-scaled chromitite layering, interlayering of peridotites, dunites, anorthosites, and chromitites all suggest that the original rocks were part of a layered sequence. Sequences similar to this are best represented today by continental layered intrusions such as the Skaergaard, Bushveld (Visser and Von Gruenewaldt, 1970) and Stillwater (Czamanske and Zientek, 1985) complexes. Although nowhere near as complete as these well-preserved complexes, the ultramafic rocks of the Sterrett area demonstrate many similarities. The Sterrett rocks, although dismembered and highly altered, are thought to have originated in a fractionating magma chamber underlying the Iapetus Ocean floor. The closing of this ocean was what produced the sequence

observable today, the deformational and metamorphic remnants of an Ordovician ocean crust emplaced upon a continental margin.

This interpretation for the Sterrett area rocks is not unique, since recent dredging of the present ocean floors and rift zones indicates suites of rocks similar to those found at Sterrett (Engel and Fisher, 1975; Bonatti et al., 1986; Rona et al., 1987).

### Metamorphic History

Hydration to produce serpentine from the original igneous mineralogy is the most obvious metamorphic event. In the Sterrett area this hydration process is essentially complete. Further northward in the Quebec ultramafic belt, however, the gradual transition of olivine, orthopyroxene and clinopyroxene to serpentine is observable. Recent work (Kimball et al., 1985) suggests that serpentinization commences at temperatures of 600°C or greater and continues to 50°C or less. This temperature interval does not confine well the temperature of alteration, as all parts of this interval probably contributed to the total serpentinization observed at Sterrett. Some of the non-serpentine assemblages do allow one to trace part of the metamorphic path and to look at stages of the evolutionary petrologic path.

Roeder et al. (1979) have presented a geothermometer based upon the Fe-Mg exchange equilibria between olivine and spinel. This geothermometer, using analyzed pairs of chromite and olivine inclusions from the Sterrett area, gives temperatures that range from 550°C to 610°C. This temperature is significantly lower than that found for crystallizing olivine-spinel from a magma and must represent a temperature of re-equilibration during metamorphism.

The subassemblage prehnite, zoisite, grossular, pumpellyite and chlorite, with or without quartz, found in the meta-anorthosite can be modeled in the system  $Al_2O_3$ -MgO-CaO (Fig. 30). A Schreinemakers' analysis of this system produces four metamorphic reactions amongst the phases (Fig. 31). Since the five phases coexist, they must have formed close to the invariant point of the petrogenetic grid. This invariant point can be located with respect to the pressure and temperature from the experimental work of Liou (1971) who determined the stability of the reaction: Prehnite = Zoisite + Grossular + Quartz +  $H_2O$  and Schiffman and Liou (1980) who found the stability curve for the reaction: Mg-Al-pumpellyite = Zoisite + Grossular + Chlorite + Quartz. These are two of the four reactions that define the petrogenetic grid of the meta-anorthosite assemblage and which place the invariant point near 380°C and 6.5 Kb (Fig. 32). The analyzed minerals of the assemblage are not far from the pure endmember phases. The analyses show that Mn partitions into garnet and  $Fe^{3+}$  into zoisite. The small amount of  $Fe^{2+}$  in pumpellyite would reduce pumpellyite's field of stability (Trzcinski and Birkett, 1982). The solid solution effects of the participating phases would tend to expand the fields of stability of the reaction products and therefore shift the reaction curves toward lower temperature and higher pressure. The relatively high pressure of metamorphism (>6Kb) accords well with the blue amphibole cores that are found in the amphibole-bearing "granitic" rocks found elsewhere within the ultramafic belt. The importance of these metamorphic conditions is the evidence that these rocks were not only subjected to near-surface conditions but that they have at some point in their history been buried to depths of 20 Km or more. Burial of these ultramafic rocks to significant depths is consistent with deep burial postulated for other parts of the Quebec ultramafic belt (Feininger, 1981; Trzcinski, 1986).

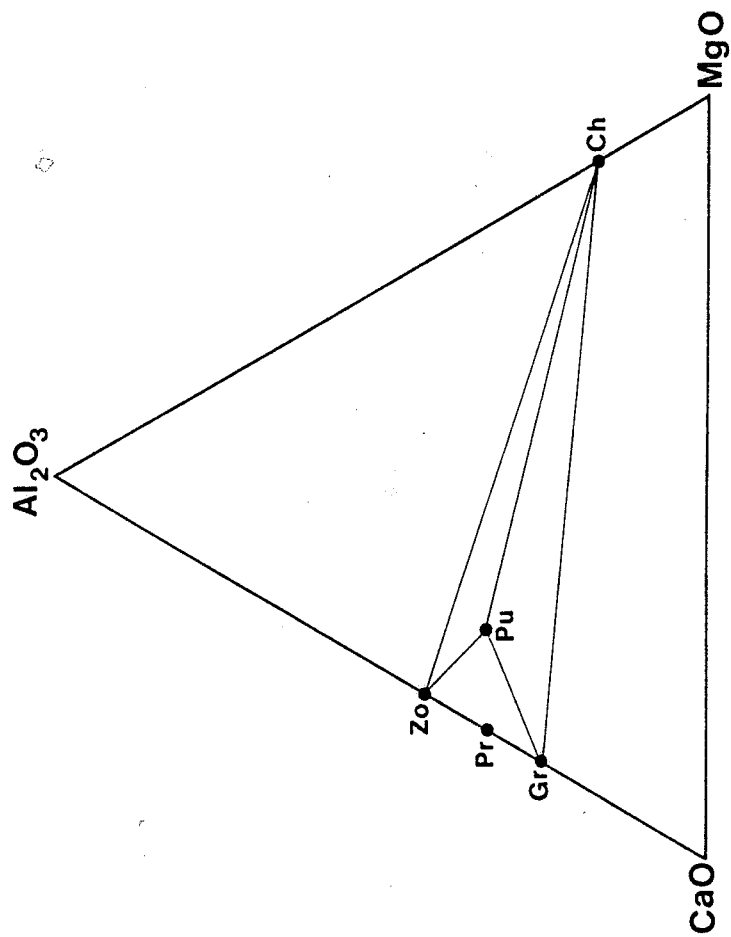


Figure 30: The system  $\text{Al}_2\text{O}_3$ - $\text{MgO}$ - $\text{CaO}$  and the phases zoisite, prehnite, pumpellyite, grossular and chlorite.



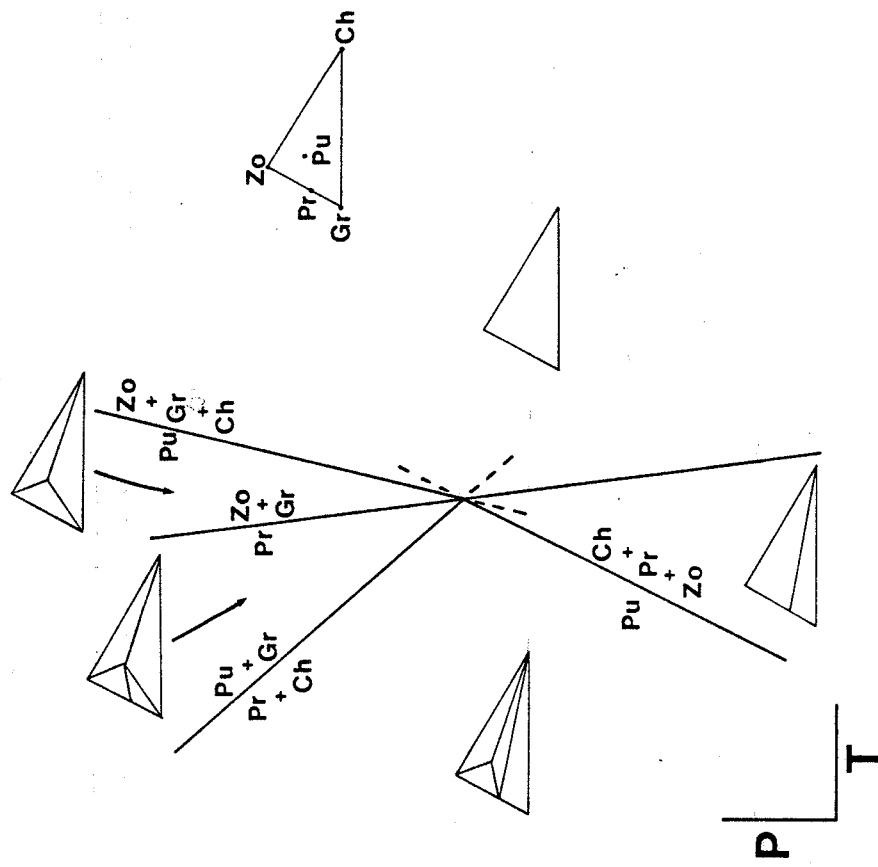
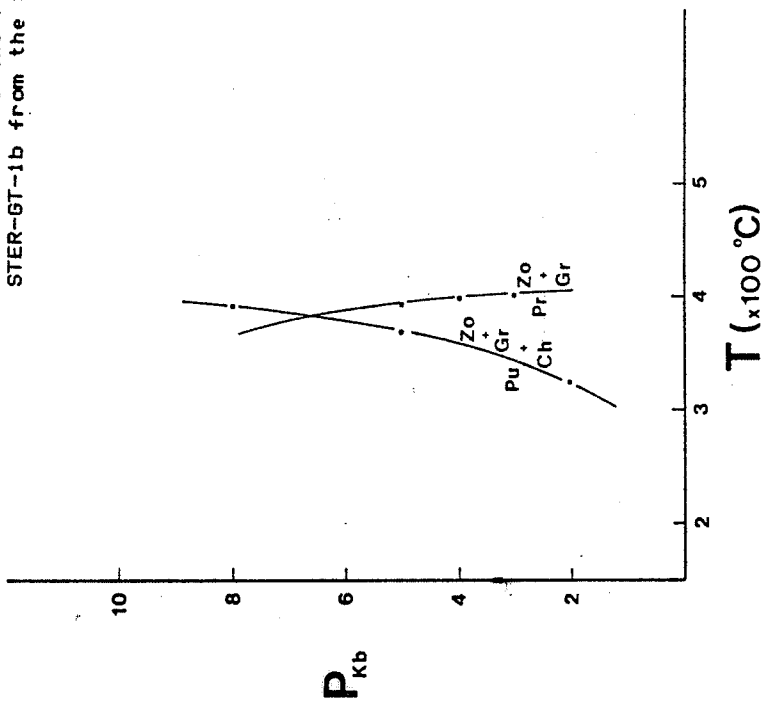


Figure 31: A Schreinemakers' analysis of the system in Fig. 30 with respect to pressure and temperature.

Figure 32: The experimentally determined curves for the reactions Prehnite = Zoisite + Grossular (Liou, 1971) and Mg-Al-pumpellyite + Zoisite + Grossular + Chlorite (Schiffman and Liou, 1980) used to define the P-T conditions of assemblage STER-GT-1b from the Sterrett mine area.



The final stage of alteration occurred when the rocks were brittle, relatively cold and not highly loaded. The slickensided fault surfaces and chrysotile fiber growth on these surfaces and in rock fractures are vestiges of this last event.

## CONCLUSIONS

The rocks of the Sterrett mine area represent a suite of layered ultramafic rocks not greatly unlike those found in the ultramafic portions of layered intrusions like the Skaergaard, Bushveld and Stillwater or those on modern ocean floors. The Sterrett rocks were transported from their oceanic mantle environment during the closure of the Iapetus ocean which has led to their deformation, metamorphism and emplacement on a continental margin.

In spite of these disruptions, these rocks are host to large concentrations of chromite that are found in a more or less continuous band in the Sterrett area. Old mine records indicate that significant tonnages of chromite have been extracted from the mine during the periods of the two world wars (Jerrom, 1951; Way and Lacaille, 1953). Chemical analyses of chromite (Appendix I) indicate that the chromite is of high commercial quality i.e. a high Cr/Fe ratio. Structural details and outcrop pattern show that the chromite-rich horizon is a vertically dipping layer that has undergone brittle deformation, with extension in the vertical direction.

Drill records and underground mining suggest that the chromite from the Sterrett property is far from exhausted, and that significant chromite may be found along strike of the chromite-rich layer as well as vertically down-dip parallel to the layering (Lacaille, 1958).

Because overburden in the area is thin, a series of gravity survey lines, perpendicular to the chromitite trend, could help delineate potential unexploited chromite-rich areas. This would be particularly important in the area between Pit B and the north end of Pit A where chromitite has been found but not been exploited. The old mine records also indicate that in the underground workings, the full potential for chromitite was never exploited to any extent north of Pit B.

Following a gravity survey a series of drill holes in a fan pattern drilled at several different stations along strike of the chromitite-rich horizon could further define the chromite-rich horizon.

Preliminary data show that in several places, PGE values are significantly above background levels. Further detailed sampling and analyses should be done in those areas showing above background values to fully evaluate PGE potential.

Observations near the Sterrett mine suggest several possible associations that may serve as guides in the exploration for other chromitite localities in the Quebec ultramafic belt, including:

The "mackerel-striped" texture of the serpentinized dunite associated with chromitite layers; the occurrence of meta-anorthosite layers near or within chromitite; the association of asbestos-rich rock to the west of the chromitite bands; and, the association of "granitic" rocks with the chromitites and asbestos-rich rocks.

## ACKNOWLEDGEMENTS

This work was carried out under contract with the Geological Survey of Canada. Assistance in the field was provided by Anne Préfontaine, Isabelle Robillard and Nathalie Marchildon. The Scientific Authority responsible for supervising the contract was Tyson C. Birkett. The typescript of this report was read and edited by R.F.J. Scoates, T.C. Birkett and D.G. Richardson (all of the Geological Survey of

Canada). D.G. Richardson also prepared the text, figures and appendices for Open Filing.

## REFERENCES

Arthaud, F., 1969, Méthode de détermination graphique des directions de reccourcissement, d'allongement et intermédiaire d'une population de failles, Bulletin Société Géologique Française, v. 11, pp. 729-737.

Bonatti, E., Ottenello, G. and Hamlyn, P.R., 1986, Peridotites from the Island of Zabagard (St. John), Red Sea: Petrology and geochemistry, Journal of Geophysical Research, v. 91, pp. 599-631.

Cooke, H.C., 1950, Geology of a southeastern part of the Eastern Townships, Quebec, Geological Survey of Canada, Memoir 257, 142 p.

Czamanske, G.K. and Zientek, M.L., 1985, The Stillwater Complex, Montana: Geology and Guide, Special Publication 92, Montana College of Mineral Science and Technology, 396 p.

Dennis, B.T., 1932, The chromite deposits of the Eastern Townships of the Province of Quebec, Annual report of the Quebec Bureau of Mines, Part D, 106 p.

Durney, D.W. and Ramsay, J.G., 1973, Incremental strains measured by syntectonic crystal growths, in Gravity and Tectonics?

DeJong, K.A. and Scholten, R., editors, John Wiley, New York, pp. 67-96. Engel, C.G. and Fisher, R.L., 1975, Granitic to ultramafic rock complexes of the Indian Ocean ridge system, western Indian Ocean, Bulletin Geological Society of America, v. 86, pp. 1553-1578.

Evans, B.W. and Frost, B.R., 1975, Chrome-spinel in progressive metamorphism--a preliminary analysis, Geochimica et Cosmochimica Acta, v. 39, pp. 959-972.

Feininger, T., 1981, Amphibolite associated with the Thetford Mines ophiolite complex at Belmina Ridge, Quebec, Canadian Journal of Earth Sciences, v. 18, pp. 1878-1892.

Jerrom, C.J., May 23, 1951, "Report of the Sterrett Chromite Property, St. Cyr, Quebec", 17p. and Appendices.

Kimball, K.L., Spear, F.S. and Dick, H.J.B., 1985, High-temperature alteration of abyssal ultramafics from the Islas Orcadas Fracture Zone, South Atlantic, Contributions to Mineralogy and Petrology, v. 91, pp. 307-320.

Lacaille, G.E., March, 1958, "Report on the Economics of the St. Cyr Chromite Mine of Albert metals Corporation Limited, St. Cyr, Cleveland Township, P.Q." 10p.

Liou, J.G., 1971, Synthesis and stability relations of prehnite,  $\text{Ca}_2\text{Al}_2\text{Si}_3\text{O}_{10}(\text{OH})_2$ , The American Mineralogist, v. 56, pp. 507-531.

Marquis, R. 1986, Géologie de la région de Richmond--Cantons de Cleveland, Kingsey et Shipton, Ministère de l'Énergie et des Ressources, Québec, MB 86-31, 56 p.

Mullins, W.J. and McQuat, J.F., November 9, 1976, "Pathfinder Resources Limited: A Report on the Lili Asbestos/Chromite Property, Cleveland Township, Richmond County, Quebec", 106p.

- Roeder, P.L., Campbell, I.H., and Jamieson, H.E., 1979, A reevaluation of the olivine-spinel geothermometer, *Contributions to Mineralogy and Petrology*, v. 68, pp. 325-334.
- Rona, P.A., Widenfolk, L., and Bostrom, K., 1987, Serpentinized ultramafics and hydrothermal activity at the Mid-Atlantic Ridge Crest near 15°N, *Journal of eophysical Research*, v. 92, pp. 1417-1427.
- Schiffman, P. and Liou, J.G., 1980, Synthesis and stability relations of Mg-Al-pumpellyite,  $\text{Ca}_4\text{MgAl}_5\text{Si}_6\text{O}_{21}(\text{OH})_7$ , *Journal of Petrology*, v. 21, pp. 441-474.
- St Julien, P. and Hubert, C., 1975, Evolution of the Taconian Orogen in the Quebec Appalachians, *American Journal of Science*, v. 275-A, pp. 337-362.
- Stockwell, C.H., 1944, Chromite deposits of the Eastern Townships, Quebec, *Canadian Institute of Mining and Metallurgy Bulletin*, v. 47.
- Thayer, T.P., 1960, Some critical differences between alpine-type and stratiform peridotite-gabbro complexes. *International Geological Congress 21st, Copenhagen, Rept. XIII*, pp. 247-249.
- Thayer, T.P., 1970, Chromite segregations as petrogenetic indicators: *Geological Society of South Africa Special Publication 1*, pp. 380-389.
- Trzcienski, W.E., Jr., 1986, Disequilibrium textures: Petrologic indicators of convergent P-T paths, Shickshock Mountains, Northern Gaspe, Quebec, Canada, *Abstracts with Programs, Geological Society of America*, v. 18, p. 73.
- Trzcienski, W.E., Jr. and Birkett, T.C., 1982, Compositional variations of pumpellyite along the western margin of the Quebec Appalachians, *Canadian Mineralogist*, v. 20, pp. 203-209.
- Visser, D.J.L. and Von Gruenewaldt, G., 1970, Symposium on the Bushveld Igneous Complex and other layered intrusions, the Geological Society of South Africa, *Special Publication 1*, 763 p.
- Way, H.G. and Lacaille, G.E., November 25, 1953, "Report Covering Lots 7, 8, 9 and 10, Range X, Cleveland Township, Richmond County", 5p.

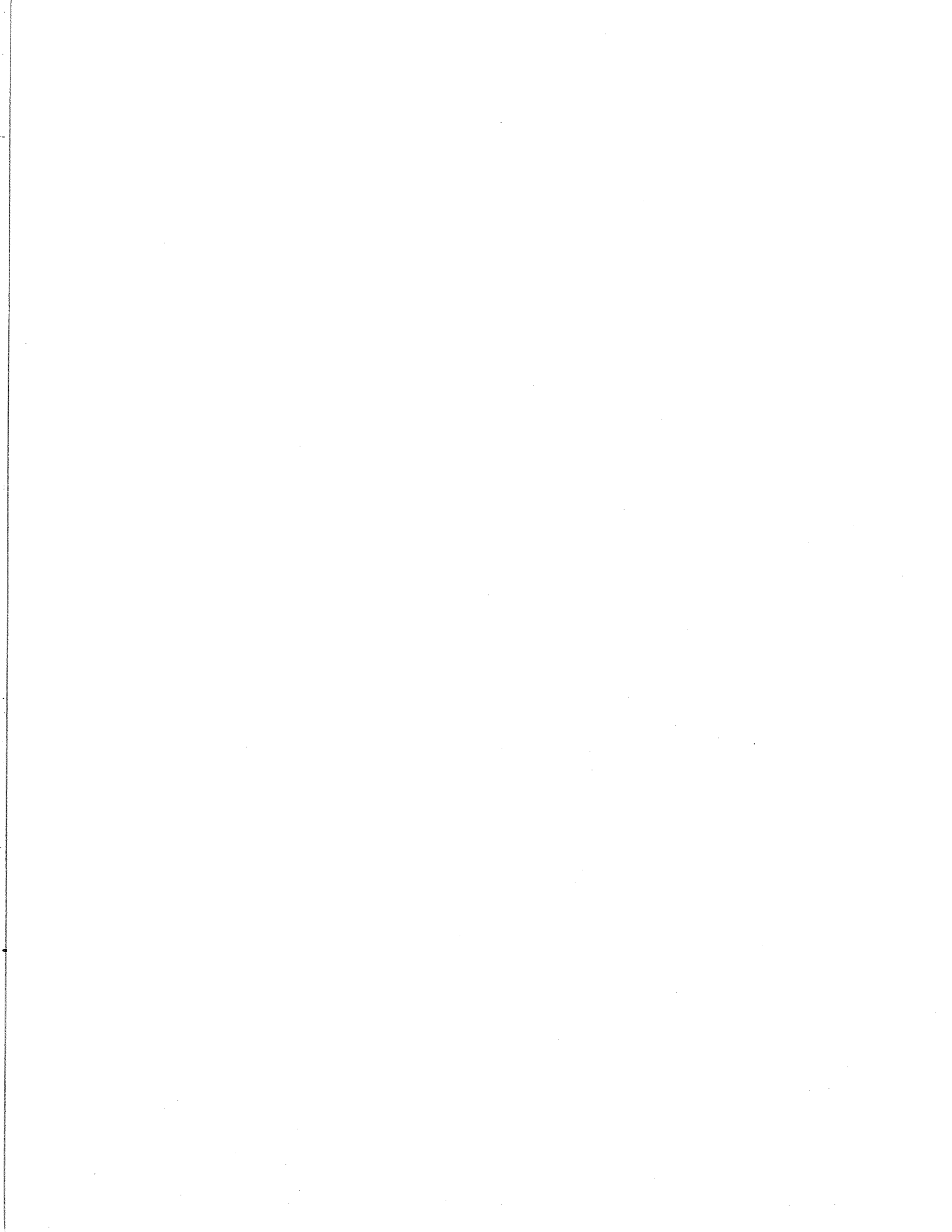
APPENDIX I

MICROPROBE ANALYSES OF MINERALS FROM THE STERRETT CHROMITE MINE  
AREA

---

MINERAL ABBREVIATIONS USED IN THE APPENDIX

AB	Albite
AMPH	Amphibole
BIO	Biotite
CHL	Chlorite
CHR	Chromite
CPX	Clinopyroxene
DIOP	Diopside
GARN	Garnet
KSPAR	K-Feldspar
MAG	Magnetite
OL	Olivine
PHLOG	Phlogopite
PLAG	Plagioclase
PREH	Prehnite
PUMP	Pumpellyite
PYRO	Pyrophanite
SERP	Serpentine
UV	Uvarovite
WM	White Mica
ZO	Zoisite



STER-1A

	#1	#2	#3	#4	#5	#6	#8	#9	#10
	PYRO	PYRO	PYRO	PYRO	PYRO	MFG	CHL	SERP	CHL
S102	1.28	.25	.19	.07	1.66	1.25	35.34	42.00	36.33
T102	52.49	53.18	54.43	54.09	51.42	.67	.00	.00	.00
R1203	.27	.00	.00	.02	.13	.10	13.60	2.27	14.06
Fe203	.00	.00	.00	.00	.00	.00	.00	.00	.00
Cr203	.00	.00	.00	.02	.00	.06	.00	.00	.00
V203	.32	.37	.37	.32	.28	.00	.00	.00	.00
F60	11.86	11.20	17.74	.46	.99	89.43	6.82	2.35	3.62
MnO	32.03	33.90	25.07	46.84	44.54	.54	.07	.00	.00
NiO	.02	.04	.04	.02	.03	.08	.00	.00	.00
MgO	2.63	1.33	3.34	.07	2.61	1.88	33.26	40.38	36.28
CaO	.01	.02	.01	.01	.00	.03	.00	.00	.00
Na2O	.00	.00	.00	.00	.00	.00	.00	.00	.00
K2O	.00	.00	.00	.00	.00	.00	.00	.00	.00

STER-GT-1A

	#1	#2	#3	#4	#5	#6	#7
	OL	OL	CHR	CHR	CHR	CHR	CHR
S102	41.61	41.14	.02	.02	.02	.03	.01
T102	.02	.00	.06	.13	.14	.18	.17
R1203	.00	.00	15.18	15.26	14.50	14.66	14.41
Fe203	.75	.94	54.69	54.31	56.14	56.19	54.82
V203	.00	.00	.00	.00	.00	.00	.00
F60	3.64	3.59	17.28	17.45	16.76	17.16	17.77
MnO	.04	.07	.40	.37	.45	.44	.40
NiO	.71	.62	.13	.08	.08	.12	.13
MgO	53.34	52.86	13.62	13.50	13.30	13.35	13.09
CaO	.02	.01	.01	.01	.00	.02	.00
Na2O	.00	.00	.00	.00	.00	.00	.00
K2O	.00	.00	.00	.00	.00	.00	.00

STER-GT-1A SULPHIDES

	#1	#2
S	31.71	32.92
Ni	43.22	36.98
Fe	12.31	16.00
Cu	.00	.00



STER-1B

	#1	#2	#3	#4	#5	#6	#7	#8	#9	#10	#11	#12	#13	#14	#15	#18	#28	#38	#48	#58
	CHR	MFG	MFG	CHR	CHR	CHR	CHR	CHR	CHR	CHR	CHR	MFG	MFG	MFG	MFG	MAG	CHR	CHR	CHR	CHR
S102	.04	2.66	.10	.05	.02	.01	.01	.05	.09	.03	4.93	1.01	.35	.50	.21	.11	.04	.04	.03	.04
T102	.02	.00	.02	.06	.07	.05	.07	.06	.07	.05	.06	.00	.00	.00	.00	.03	.07	.05	.05	.09
AL203	9.03	.01	1.46	9.19	9.49	9.73	9.82	9.76	9.33	8.91	8.01	.02	.01	.00	.00	.03	9.77	8.00	7.98	8.06
Fe203	.00	.00	.00	.00	.00	.00	.00	.00	.00	.00	.00	.00	.00	.00	.00	.00	.00	.00	.00	.00
Cr203	61.22	1.00	18.80	60.77	62.11	61.56	62.58	62.54	62.75	61.89	30.19	1.60	1.18	.06	.70	11.00	59.95	63.17	62.06	63.34
V203	.00	.00	.00	.00	.00	.00	.00	.00	.00	.00	.00	.00	.00	.00	.00	.00	.00	.00	.00	.00
Fe0	20.02	85.67	79.65	17.37	16.98	15.62	14.76	14.12	15.00	18.45	34.57	86.79	88.97	88.05	89.81	89.43	19.73	18.61	17.63	17.20
Ni0	.45	.22	.39	.41	.34	.24	.36	.30	.35	.37	.76	.23	.20	.20	.29	.22	.48	.40	.40	.37
Ni10	.30	.87	.36	.04	.10	.05	.05	.06	.04	.07	.13	.76	.68	.71	.68	.67	.00	.09	.09	.00
Pg0	9.47	7.11	4.20	11.23	11.67	12.44	13.31	13.21	13.05	10.19	14.84	1.26	1.16	.75	.36	.49	9.89	10.45	10.59	11.20
Ca0	.01	.03	.00	.02	.00	.00	.00	.02	.02	.00	.02	.00	.02	.02	.00	.00	.01	.00	.00	.01
Na20	.00	.00	.00	.00	.00	.00	.00	.00	.00	.00	.00	.00	.00	.00	.00	.00	.00	.00	.00	.00
K20	.00	.00	.00	.00	.00	.00	.00	.00	.00	.00	.00	.00	.00	.00	.00	.00	.00	.00	.00	.00

STER-1B SULFIDES

	#1	#2	#3	#4	#5	#6	#7	#8	#9	#10	#11	#12	#13	#14	#15	#16	#17	#18	#19	#20
S	27.12	26.89	27.17	27.23	27.10	27.01	27.41	27.45	27.60	27.32	27.41	27.22	12.90	26.51	27.35	27.66	27.42	27.50	27.39	42.46
Ni	72.88	73.60	72.39	72.94	71.65	72.47	69.92	71.06	71.10	70.43	71.34	70.70	34.06	70.43	68.24	66.82	68.55	66.62	67.28	102.95
Fe	.10	.02	.03	.07	.12	.14	.16	.00	.01	.06	.06	.09	8.02	.26	.05	.04	.01	.00	.11	.02
Cu	.00	.00	.00	.14	.00	.00	.00	.00	.00	.02	.00	.01	.00	.04	.00	.00	.00	.00	.00	.00
Zn	.00	.05	.03	.00	.00	.06	.05	.00	.00	.00	.00	.00	.11	.00	.07	.01	.12	.00	.03	.01
S	.00	34.84	27.45	27.57	27.52	27.71	27.49	26.87	27.12	27.51	27.37	27.40	27.40	27.27	26.89	26.95	27.67			
Ni	66.59	.00	73.04	72.46	73.13	72.55	73.22	72.11	72.70	73.28	72.69	72.70	73.18	72.26	73.03	72.63	72.94			
Fe	.01	30.10	.10	.22	.19	.00	.02	.00	.00	.00	.03	.00	.00	.43	.17	.07	.24			
Cu	.04	34.60	.00	.00	.00	.00	.00	.00	.00	.00	.02	.00	.00	.00	.03	.06	.00			
Zn	.00	.08	.00	.07	.05	.00	.00	.00	.00	.00	.04	.06	.01	.00	.00	.00	.12			



STER-67-1B

SULFIDES

	#1	#2	#3	#1B	#2B	#3B	#4B	#5B	#6B	#7B
S	26.81	1.48	15.05	26.48	26.97	26.53	26.53	30.86	26.90	28.06
Ni	74.15	3.98	42.05	73.17	72.95	73.00	73.19	68.38	73.26	71.95
Fe	.09	1.56	.85	.05	.14	.10	.28	.06	.01	.08
Cu	.00	.04	.02	.00	.00	.00	.00	.00	.00	.00
Zn	.00	.00	.00	.06	.03	.00	.14	.01	.05	.00

STER-GT-2R

	#1	#2	#3	#4	#5	#6	#7	#8	#9	#10	#11	#12
	OL	OL	OL	OL	OL	OL	OL	CHR	CHR	CHR	CHR	CHR
SiO2	40.90	41.09	41.09	41.09	40.82	40.73	41.88	.06	.02	.02	.02	.04
TiO2	.00	.00	.00	.00	.00	.00	.00	.10	.13	.11	.10	.10
Al2O3	.00	.00	.00	.00	.00	.00	.00	14.02	14.65	14.81	13.49	14.60
Fe2O3	.00	.00	.00	.00	.00	.00	.00	.00	.00	.00	.00	.00
Cr2O3	.12	.08	.09	.09	.09	.29	.56	54.58	54.38	54.07	56.49	54.18
V2O3	.00	.00	.00	.00	.00	.03	.02	.08	.12	.08	.14	.10
FeO	4.97	5.15	5.19	5.36	5.15	4.89	4.29	18.23	18.74	18.47	17.41	19.78
MnO	.08	.07	.08	1.10	.05	.08	.03	.11	.11	.14	.14	.16
NiO	.93	1.06	1.06	1.02	1.02	1.03	1.19	.13	.18	.16	.06	.12
MgO	52.41	52.64	52.61	52.79	52.94	52.94	53.60	12.32	12.34	12.50	12.39	11.87
CaO	.02	.02	.02	.06	.01	.01	.00	.00	.00	.00	.00	.00
Na2O	.00	.00	.00	.00	.00	.00	.00	.00	.00	.00	.00	.00
K2O	.00	.00	.00	.00	.00	.00	.00	.00	.00	.00	.00	.00

	#13	#14	#15	#16	#18	#19	#20	#21	#22	#23
	CHR	CHR	PYR	PYR	PHLOG	PHLOG	PHLO	PHLOG	CHL	CHL
SiO2	.06	.02	.48	.62	38.09	37.66	39.22	37.79	33.54	30.39
TiO2	.28	.13	51.66	52.14	.60	.64	.58	.48	.30	.15
Al2O3	5.43	15.94	.32	.25	16.17	16.15	15.58	14.84	8.95	16.02
Fe2O3	.00	.00	.00	.00	.00	.00	.00	.00	.00	.00
Cr2O3	61.04	53.44	.00	.00	.15	.14	.70	.52	1.57	.55
V2O3	.18	.12	.32	.33	.00	.00	.00	.00	.00	.00
FeO	26.37	17.49	28.15	28.19	2.54	2.97	1.69	2.48	2.61	1.14
MnO	1.40	.12	17.27	15.77	.08	.11	.03	.05	.11	.00
NiO	.14	.05	.04	.04	.00	.00	.00	.00	.00	.00
MgO	7.40	12.79	1.70	1.17	23.83	24.20	24.52	25.94	35.34	33.55
CaO	.00	.00	.04	.05	.01	.05	.00	.00	.00	.00
Na2O	.00	.00	.00	.00	1.34	1.12	.60	.00	.00	.01
K2O	.00	.00	.00	.00	7.40	7.17	8.77	8.03	.00	.45





STER-68

	#1	#2	#3	#4	#5	#6	#7	#8	#9	#10	#11	#12	#13	#14	#15	#16	#17
	CHR	CHR	MAG	CHR	CHR	CHR	CHR	MAG	MAG	MAG	MAG	MAG	DIOP	MAG	SERP	SERP	SERP
SiO2	.04	.05	.07	.06	.02	.04	.03	.07	.10	.07	.08	.18	53.97	.07	42.50	40.85	43.03
TiO2	.22	.18	.06	.21	.18	.20	.20	.07	.06	.06	.08	.06	.00	.06	.00	.00	.00
Al2O3	16.21	16.26	.00	14.91	16.14	16.34	16.46	.00	.00	.00	.00	.00	.10	.00	.07	.12	.05
Fe2O3	.00	.00	.00	.00	.00	.00	.00	.00	.00	.00	.00	.00	.00	.00	.00	.00	.00
Cr2O3	52.06	52.19	1.72	49.88	51.44	50.82	50.89	2.79	.68	.45	.25	.19	1.63	.18	.08	.06	.07
V2O5	.11	.14	.00	.11	.12	.13	.13	.02	.03	.03	.00	.03	.00	.05	.02	.02	.00
FeO	18.25	18.50	90.41	20.53	18.52	18.79	19.57	90.58	91.60	91.28	90.93	88.45	.47	91.34	1.42	1.94	1.71
MnO	.15	.19	.02	.18	.11	.15	.16	.04	.00	.00	.00	.00	.00	.00	.04	.03	.03
NiO	.13	.10	.27	.12	.09	.10	.10	.26	.28	.31	.35	.37	.00	.37	.10	.72	.11
MgO	12.92	12.92	.37	11.92	12.93	12.92	12.92	.35	.34	.29	.30	.44	17.48	.53	39.43	39.12	39.19
CaO	.02	.00	.00	.01	.00	.01	.00	.04	.03	.04	.04	.04	24.90	.03	.00	.04	.00
Na2O	.00	.00	.00	.00	.00	.00	.00	.00	.00	.00	.00	.00	.00	.00	.00	.00	.00
K2O	.00	.00	.00	.00	.00	.00	.00	.00	.00	.00	.00	.00	.00	.00	.00	.00	.00

Ster-3C

	#1	#2	#3	#4	#5	#6	#7	#8	#9	#10	#11	#12
	OL	OL	DIOP	DIOP	CHR	CHR	CHR	CHR	CHR	CHR	CHR	CHR
SiO2	40.82	41.64	54.05	53.19	.03	.05	.03	.05	.05	.04	.03	.14
TiO2	.00	.00	.07	.07	.17	.18	.17	.16	.17	.14	.17	.18
Al2O3	.00	.00	.97	.85	14.90	14.84	14.36	14.80	15.19	15.18	14.53	15.90
Fe2O3	.00	.00	.00	.00	.00	.00	.00	.00	.00	.00	.00	.00
Cr2O3	.22	.44	.91	.83	55.17	55.07	55.45	54.21	54.16	53.89	55.05	53.32
V2O5	.00	.00	.00	.00	.13	.09	.08	.11	.13	.11	.11	.14
FeO	3.35	3.28	1.07	1.10	14.27	14.90	15.08	15.58	15.69	15.71	15.67	16.22
MnO	.05	.03	.03	.02	.13	.15	.12	.16	.12	.14	.17	.12
NiO	.53	.52	.05	.10	.05	.05	.05	.04	.07	.07	.07	.08
MgO	54.07	54.95	17.90	17.81	15.36	14.96	14.68	14.57	14.81	14.70	14.71	14.88
CaO	.02	.00	25.22	25.24	.00	.00	.00	.13	.17	.00	.00	.06
Na2O	.00	.00	.00	.00	.00	.00	.00	.00	.00	.00	.00	.00
K2O	.00	.00	.00	.00	.00	.00	.00	.00	.00	.00	.00	.00
Total	99.06	100.86	100.27	99.21	100.21	100.29	99.99	99.81	100.56	99.98	100.51	101.04

STER-51

	#1	#2	#3	#4	#5	#6	#7	#8	#9	#10	#11	#12	#13	#14	#15	#16	#17	#18
	OL	OL	OL	OL	OL	OL	OL	CHR	CHR	CHR	CHR	CHR	CHR	CHR	CHR	CHR	CHR	CHR
SiO2	40.84	41.00	40.92	41.14	40.85	41.07	41.41	.00	.03	.03	.00	.05	.00	.00	.02	.02	.00	.00
TiO2	.00	.00	.00	.02	.00	.00	.02	.13	.13	.13	.00	.14	.13	.12	.12	.12	.00	.12
Al2O3	.00	.00	.01	.00	.02	.02	21.49	21.08	21.43	22.58	21.65	21.65	21.32	21.31	21.54	21.31	21.32	22.02
Fe2O3	.03	.08	.34	.32	.59	.23	48.13	47.67	48.17	46.96	47.70	47.70	47.21	47.85	47.12	47.85	47.83	47.99
Cr2O3	.00	.00	.00	.00	.00	.00	.00	.15	.12	.15	.16	.16	.16	.17	.15	.14	.12	.17
V2O3	4.38	4.30	3.55	3.43	3.50	4.11	3.60	15.81	15.85	15.75	14.91	14.91	15.70	15.23	15.20	15.81	15.41	15.41
FeO	.07	.06	.06	.05	.05	.05	.05	.11	.09	.09	.12	.08	.11	.12	.07	.10	.12	.08
MnO	.50	.47	.59	.61	.61	.51	.55	.05	.06	.05	.05	.08	.13	.07	.05	.05	.06	.07
NiO	53.62	53.23	54.95	54.42	54.10	53.86	55.03	15.18	15.01	15.25	15.39	15.46	15.06	15.22	15.28	15.02	15.15	15.39
MgO	.09	.08	.02	.03	.02	.10	.02	.00	.02	.01	.00	.01	.01	.00	.00	.00	.00	.00
CaO	.00	.00	.00	.00	.00	.00	.00	.00	.00	.00	.00	.00	.00	.00	.00	.00	.00	.00
Na2O	.00	.00	.00	.00	.00	.00	.00	.00	.00	.00	.00	.00	.00	.00	.00	.00	.00	.00
K2O	.00	.00	.00	.00	.00	.00	.00	.00	.00	.00	.00	.00	.00	.00	.00	.00	.00	.00

STER-40

	#1	#2	#3	#4	#5	#6	#7	#8	#9	#10	#11	#12	#13	#14	#15	#16	#17	#18
	CHR	SERP	OL	OL	OL	CHR	CHR	CHR	CHR	SERP	CHR	CHR	CHR	CHR	CHR	CHR	CHR	CHR
SiO2	.02	44.91	42.76	42.71	42.70	.02	.01	.06	.03	44.11	.03	.01	.03	.02	.00	.01	.00	.00
TiO2	.24	.14	.00	.05	.20	.13	.26	.23	.08	.04	.23	.21	.25	.70	.14	.19	.12	.12
Al2O3	15.17	.27	.00	.01	.00	15.31	15.52	15.44	14.99	.50	15.10	15.24	15.07	.68	12.60	12.49	.00	.00
Fe2O3	.00	.00	.00	.00	.00	.00	.00	.00	.00	.00	.00	.00	.00	.00	.00	.00	.00	.00
Cr2O3	56.04	.62	.41	.59	.35	55.81	56.45	56.01	57.02	.32	56.22	56.22	56.07	.00	39.32	39.11	.00	.00
V2O3	.00	.00	.00	.00	.00	.00	.00	.00	.00	.00	.00	.00	.00	.00	.00	.00	.00	.00
FeO	16.98	3.03	4.03	3.85	4.24	16.75	16.28	16.65	17.08	2.20	17.23	17.89	17.54	40.46	16.66	16.56	.00	.00
MnO	.46	.00	.05	.08	.01	.40	.45	.55	.50	.00	.58	.52	.46	1.92	1.33	1.36	.00	.00
NiO	.00	.00	.00	.00	.00	.00	.00	.00	.00	.00	.00	.00	.00	.00	.00	.00	.00	.00
MgO	14.17	40.90	53.42	54.02	53.50	14.21	14.49	14.03	13.74	39.37	13.49	13.27	13.34	.87	11.31	11.27	.00	.00
CaO	.00	.02	.01	.02	.00	.01	.00	.02	.00	.05	.00	.00	.00	.03	.00	.00	.00	.00
Na2O	.00	.00	.00	.00	.01	.01	.00	.02	.00	.01	.00	.01	.00	.07	.00	.00	.00	.00
K2O	.00	.01	.00	.00	.00	.00	.00	.00	.00	.00	.01	.00	.00	.00	.00	.00	.00	.00

SULFIDES

	#1	#2
S	29.65	29.80
Ni	40.86	40.79
Fe	20.18	20.73
Cu	.00	.00
Zn	.05	.00



C-2-D

	#1	#2	#3	#4	#1B	#2B	#3B	#4B	#5B	#6B	#7B	#8B	#9B	#10B	#11B	#12B	#13B	#14B	#15B
	CHR	CHR	CHR	CHR	CHR	CHR	CHR	CHR	CHR	CHR	CHR	CHR	CHR	CHR	CHR	CHR	CHR	CHR	CHR
Si02	.06	.04	.04	.04	.04	.04	.03	.06	.02	.10	.01	.01	.07	.25	.03	.02	.02	.04	.03
Ti02	.04	.28	.03	.05	.05	.03	.03	.03	.04	.06	.01	.02	.06	.06	.05	.04	.04	.04	.04
Al2O3	22.84	22.92	22.92	22.89	15.77	7.92	16.40	16.29	16.08	8.35	.00	3.16	12.17	2.73	16.40	16.18	16.22	16.10	16.26
Fe2O3	.00	.00	.00	.00	.00	.00	.00	.00	.00	.00	.00	.00	.00	.00	.00	.00	.00	.00	.00
Cr2O3	47.12	48.30	46.62	47.52	53.02	59.52	53.56	53.07	53.50	56.11	.00	63.47	53.45	60.73	56.64	52.33	53.48	53.44	53.23
V2O5	.00	.00	.00	.00	.00	.00	.00	.00	.00	.00	.00	.00	.00	.00	.00	.00	.00	.00	.00
FeO	12.98	12.99	12.83	13.23	19.50	22.80	15.49	15.21	15.28	24.19	.08	24.36	19.74	22.87	15.81	15.38	15.40	15.55	15.33
MnO	.32	.28	.31	.44	.54	.83	.41	.41	.48	1.41	.00	.94	.61	.96	.05	.50	.38	.41	.39
NiO	.13	.20	.15	.16	.08	.06	.08	.05	.08	.02	.18	.06	.07	.00	.05	.11	.08	.13	.00
MgO	17.37	17.48	17.39	17.27	12.70	10.10	14.95	14.98	15.14	7.08	98.95	7.59	11.18	7.14	14.70	14.95	15.03	15.09	15.08
CaO	.00	.00	.00	.00	.02	.00	.00	.00	.00	.01	.07	.00	.01	.05	.01	.01	.01	.00	.00
Na2O	.00	.00	.00	.00	.00	.00	.00	.00	.00	.00	.00	.00	.00	.00	.00	.00	.00	.00	.00
K2O	.00	.00	.00	.00	.00	.00	.00	.00	.00	.00	.00	.00	.00	.00	.00	.00	.00	.00	.00

	#16B	#17B	#18B	#19B	#20B	#21B	#22B	#23B	#24B	#25B	#26B	#27B	#28B	#29B	#30B	#31B	#32B	#33B	#34B
	CHR	CHR	CHR	CHR	CHR	CHR	CHR	CHR	CHR	CHR	CHR	CHR	CHR	CHR	CHR	CHR	CHR	CHR	CHR
Si02	.03	.03	.02	.05	.03	.02	.05	.03	.03	.04	.04	60.67	62.34	.07	.03	.04	.03	.06	.02
Ti02	.07	.06	.08	.05	.06	.04	.03	.07	.04	.05	.07	.00	.00	.03	.04	.06	.07	.06	.06
Al2O3	16.13	16.18	16.08	16.23	16.14	16.13	16.00	16.07	16.06	16.20	16.05	.69	.05	15.30	15.21	15.33	3.39	15.15	15.01
Fe2O3	.00	.00	.00	.00	.00	.00	.00	.00	.00	.00	.00	.00	.00	.00	.00	.00	.00	.00	.00
Cr2O3	52.83	52.91	53.66	53.18	52.88	53.13	53.20	54.45	52.87	53.34	53.07	.40	.02	48.07	48.56	49.02	58.08	49.48	54.97
V2O5	.00	.00	.00	.00	.00	.00	.00	.00	.00	.00	.00	.00	.00	.00	.00	.00	.00	.00	.00
FeO	15.14	15.77	14.89	15.65	15.57	15.27	15.31	15.41	15.43	15.25	14.99	2.62	2.00	15.85	15.87	16.42	23.10	17.54	15.87
MnO	.35	.38	.39	.45	.45	.47	.49	.40	.46	.52	.45	.03	.03	.43	.46	.46	.72	.62	.65
NiO	.11	.14	.08	.08	.04	.14	.04	.06	.09	.12	.07	.29	.12	.00	.06	.06	.02	.01	.12
MgO	15.15	15.34	15.21	15.24	15.04	15.15	15.32	15.13	15.14	15.41	15.35	29.91	30.51	13.03	12.92	12.60	7.94	12.23	14.61
CaO	.02	.00	.00	.00	.00	.00	.02	.00	.03	.00	.00	.04	.02	.00	.00	.01	.03	.01	.03
Na2O	.00	.00	.00	.00	.00	.00	.00	.00	.00	.00	.00	.00	.00	.00	.00	.00	.00	.00	.00
K2O	.00	.00	.00	.00	.00	.00	.00	.00	.00	.00	.00	.00	.00	.00	.00	.00	.00	.00	.00

	#35B	#36B	#37B	#38B	#39B	#40B
	CHR	CHR	CHR	CHL	CHL	CHR
Si02	.03	.03	.06	32.72	33.03	.03
Ti02	.07	.04	.04	.01	.00	.07
Al2O3	16.69	15.40	16.07	13.51	13.80	6.33
Fe2O3	.00	.00	.00	.00	.00	.00
Cr2O3	52.87	48.41	53.24	3.12	3.03	61.30
V2O5	.00	.00	.00	.00	.00	.00
FeO	15.65	15.65	15.23	4.88	4.98	22.57
MnO	.58	.44	.48	.16	.21	.64
NiO	.03	.07	.03	.58	.57	.07
MgO	15.28	12.91	14.87	31.88	30.99	9.10
CaO	.02	.00	.00	.01	.03	.00
Na2O	.00	.00	.00	.00	.00	.00
K2O	.00	.00	.00	.00	.00	.00

CODD-2

	#1	#2	#3	#4	#5	#18	#28	#38	#48	#58	#6	#7	#8	#9	#10	#11	#12	#13	#14
	AMPH	AMPH	AMPH	AMPH	PLRG	PLRG	PLRG	PLRG	PLRG	PLRG	AMPH	AMPH	AMPH	AMPH	AMPH	AMPH	AMPH	AMPH	AMPH
SiO2	54.27	54.00	53.43	54.44	68.42	71.65	66.35	67.48	67.12	67.17	53.84	52.54	52.22	53.21	53.32	53.91	52.55	54.07	54.06
TiO2	.02	.05	.00	.05	.00	.00	.01	.01	.01	.00	.00	.01	.02	.02	.06	.08	.08	.08	.07
Al2O3	.55	1.11	.20	.71	19.87	20.87	19.13	19.45	19.54	19.61	.09	1.14	.22	.42	1.18	1.22	1.43	1.12	.82
Fe2O3	.00	.00	.00	.00	.00	.00	.00	.00	.00	.00	.00	.00	.00	.00	.00	.00	.00	.00	.00
Cr2O3	.10	.02	.00	.02	.00	.00	.00	.03	.00	.00	.00	.08	.07	.00	.15	.16	.13	.14	.09
V2O5	.00	.00	.00	.00	.00	.00	.00	.00	.00	.00	.00	.00	.00	.00	.00	.00	.00	.00	.00
FeO	20.79	21.53	21.23	20.86	.00	.01	.05	.02	.02	.03	19.53	19.27	20.39	20.97	20.74	21.12	22.30	21.40	19.02
MnO	.47	.48	.29	.50	.00	.00	.00	.02	.03	.02	.35	.36	.29	.24	.45	.88	.83	.84	.71
NiO	.00	.00	.00	.00	.00	.00	.00	.00	.00	.00	.00	.00	.00	.00	.00	.00	.00	.00	.00
MgO	10.53	10.37	10.49	11.08	.00	.00	.00	.00	.01	.00	11.49	9.36	10.32	10.77	10.42	13.51	13.47	11.75	12.57
CaO	10.13	7.10	12.36	6.75	.05	.21	.08	.00	.01	.24	12.60	11.52	12.51	12.38	7.17	2.35	2.58	3.97	4.97
Na2O	1.36	3.30	.11	3.82	11.93	11.05	7.59	11.54	11.95	11.65	.05	.81	.12	.16	3.50	4.01	3.12	4.40	4.64
K2O	.07	.08	.04	.14	.03	.06	.05	.04	.05	.05	.02	.05	.03	.04	.12	.04	.06	.09	.13
Total	98.27	98.04	98.15	98.37	100.30	103.85	93.26	98.99	98.74	98.80	97.97	95.34	96.19	98.21	97.11	97.28	96.68	97.86	97.08

	#15	#16	#17	#18	#19	#20	#21	#22	#23	#24	#25	#26	#27	#28	#29	#30	#31	#32	#33
	AMPH	AMPH	AMPH	AMPH	AMPH	AMPH	AMPH	AMPH	AMPH	AMPH	AMPH	AMPH	AMPH	AMPH	AMPH	AMPH	PLRG	PLRG	PLRG
SiO2	52.42	51.05	53.99	53.20	53.99	53.72	53.73	52.41	53.24	52.99	52.99	54.07	53.38	48.10	51.50	48.78	58.76	68.73	66.11
TiO2	.08	.02	.00	.01	.03	.07	.10	.13	.14	.07	.09	.02	.00	.78	.56	.19	.00	.00	.00
Al2O3	2.03	.29	.05	.28	.13	.72	1.21	1.54	1.02	.98	.78	.08	.14	6.36	4.22	5.54	19.63	19.70	19.76
Fe2O3	.00	.00	.00	.00	.00	.00	.00	.00	.00	.00	.00	.00	.00	.00	.00	.00	.00	.00	.00
Cr2O3	.09	.10	.02	.08	.22	.05	.07	.08	.07	.00	.09	.00	.03	.00	.00	.00	.00	.00	.00
V2O5	.00	.00	.00	.00	.00	.00	.00	.00	.00	.00	.00	.00	.00	.00	.00	.00	.00	.00	.00
FeO	19.35	20.28	20.66	21.60	19.45	19.64	20.73	20.78	21.30	21.28	21.80	19.63	21.42	15.79	15.47	16.94	.08	.01	.03
MnO	.36	.39	.45	.49	.31	.71	.54	.46	.56	.49	.49	.36	.38	.26	.27	.31	.02	.00	.00
NiO	.00	.00	.00	.00	.00	.00	.00	.00	.00	.00	.00	.00	.00	.00	.00	.00	.00	.00	.00
MgO	11.46	10.23	10.97	10.00	10.87	11.88	10.71	10.29	10.17	9.83	10.03	11.27	10.26	12.71	13.76	11.87	.00	.00	.00
CaO	9.66	11.81	12.30	12.29	12.44	4.24	7.50	8.74	6.40	11.77	6.81	12.39	12.53	11.63	11.95	12.14	.00	.00	.00
Na2O	2.32	.39	.06	.11	.17	5.13	2.63	2.76	4.17	4.99	3.03	1.10	.06	1.66	1.16	1.02	.02	.02	.57
K2O	.10	.13	.03	.06	.04	.09	.08	.11	.11	.08	.11	.03	.03	.21	.16	.15	11.88	11.88	11.20
Total	97.87	94.69	98.53	98.12	97.25	96.23	97.30	97.30	97.18	97.71	98.22	97.95	98.23	97.50	99.05	96.94	100.42	100.41	97.76

	#34	#35	#36
	PLRG	PLRG	PLRG
SiO2	61.96	61.36	67.85
TiO2	.00	.02	.00
Al2O3	20.54	21.96	19.69
Fe2O3	.00	.00	.00
Cr2O3	.04	.03	.00
V2O5	.00	.00	.00
FeO	.46	.27	.05
MnO	.01	.03	.02
NiO	.00	.00	.00
MgO	.21	.14	.00
CaO	.03	.05	.35
Na2O	.31	1.83	11.46
K2O	15.84	13.00	.14
Total	99.40	98.69	99.76

COND 4+00

	#1	#2	#3	#4	#5	#6	#7	#8	#9	#10	#11	#12	#13	#14	#15	#16	#17	#18
SiO2	52.35	53.15	51.62	52.36	51.83	52.11	53.32	53.43	52.64	52.44	52.41	52.81	51.78	51.56	51.89	46.49	52.49	51.92
TiO2	.15	.17	.31	.26	.21	.16	.04	.00	.00	.10	.09	.16	.20	.26	.31	7.33	.04	.18
Al2O3	.86	.89	1.69	1.28	1.17	.97	.63	2.56	.98	.69	.63	1.12	1.15	1.50	1.75	7.46	.10	1.30
Fe2O3	.00	.00	.00	.00	.00	.00	.00	.00	.00	.00	.00	.00	.00	.00	.00	.00	.00	.00
Cr2O3	.00	.00	.02	.00	.01	.00	.00	.01	.02	.02	.00	.00	.00	.00	.01	.00	.03	.00
V2O5	.00	.00	.00	.00	.00	.00	.00	.00	.00	.00	.00	.00	.00	.00	.00	.00	.00	.00
FeO	23.39	21.02	23.84	22.51	22.76	22.69	23.32	22.79	24.03	23.03	22.29	22.86	23.58	22.24	23.19	16.93	22.63	22.45
MnO	1.84	1.72	1.56	1.19	1.43	.54	.88	.61	.58	.62	.50	1.88	.66	1.24	1.88	.53	.75	1.78
NiO	.00	.00	.00	.00	.00	.00	.00	.00	.00	.00	.00	.00	.00	.00	.00	.00	.00	.00
MgO	14.20	13.57	14.12	9.96	11.84	9.30	9.35	6.76	8.01	8.57	8.62	12.75	8.01	11.74	11.62	11.01	8.47	15.02
CaO	1.27	3.10	1.47	4.38	4.41	6.74	4.69	9.43	5.87	7.90	9.18	2.23	7.97	3.80	2.91	11.12	12.42	1.30
Na2O	1.22	1.61	1.29	3.53	2.14	3.39	4.05	2.13	3.69	2.19	2.06	2.58	2.90	2.75	2.89	1.16	.09	1.20
K2O	.00	.03	.02	.09	.06	.10	.09	.07	.16	.08	.11	.05	.13	.07	.05	.19	.02	.02

	#18	#19	#20	#21	#22	#23	#24	#25	#26	#27	#28	#29	#30
SiO2	51.92	48.44	45.63	45.82	44.65	44.43	33.37	43.24	42.75	65.30	65.71	66.49	65.91
TiO2	.18	.25	.00	.00	.00	.11	.14	.00	.00	.00	.00	.00	.00
Al2O3	1.30	5.92	5.54	5.09	5.29	5.28	21.77	37.66	36.68	20.08	19.77	19.59	19.86
Fe2O3	.00	.00	.00	.00	.00	.00	.00	.00	.00	.00	.00	.00	.00
Cr2O3	.00	.02	.00	.00	.00	.00	.02	.00	.00	.00	.00	.00	.00
V2O5	.00	.00	.00	.00	.00	.00	.00	.00	.00	.00	.00	.00	.00
FeO	22.45	17.36	29.27	29.55	28.70	28.57	26.72	.28	1.08	.00	.00	.00	.00
MnO	1.78	.72	1.31	1.30	1.33	1.52	.36	.00	.02	.00	.00	.00	.00
NiO	.00	.00	.00	.00	.00	.00	.00	.00	.00	.00	.00	.00	.00
MgO	15.02	12.25	4.59	4.74	4.61	4.55	1.96	.03	.19	.00	.00	.00	.00
CaO	1.30	9.78	.09	.63	.04	.09	.03	.00	.00	.48	.21	.00	.31
Na2O	1.20	1.61	.08	.14	.03	.04	.52	.24	.18	11.25	11.26	11.71	11.03
K2O	.02	.09	.99	1.10	.95	1.18	9.67	11.09	8.06	.03	.00	.00	.02

RB-2

	#1	#2	#3	#4	#5	#6	#7	#8	#9	#10	#11	#12	#13	#14	#15	#16	#17	#18
	CHR	CHR	DIOP	AMPH	CHR	DIOP	AMPH	CHR	OL	OL	OL	OL	CHR	CHR	CHR	SERP	CHR	CHL
S102	.03	.02	53.76	44.75	.03	53.78	44.07	.03	41.33	41.06	41.37	40.80	.03	.00	-.04	43.14	.01	32.01
T102	.15	.15	.07	.48	.11	.05	.48	.17	.03	.00	.02	.00	.15	.18	.15	.00	.09	15.27
Al203	12.62	12.20	.86	10.16	12.02	.79	10.40	11.91	.01	.00	.00	.00	11.68	12.75	12.27	.12	11.83	.00
Fe203	.00	.00	.00	.00	.00	.00	.00	.00	.00	.00	.00	.00	.00	.00	.00	.00	.00	.00
Cr203	58.65	58.10	2.45	3.84	58.23	2.26	3.85	58.04	.70	.66	.71	.83	58.57	58.61	58.21	.25	59.15	2.60
U203	.00	.00	.00	.00	.00	.00	.00	.00	.00	.00	.00	.00	.00	.00	.00	.00	.00	.00
FeO	16.06	15.92	1.30	1.56	16.04	1.16	1.63	16.14	3.05	3.34	3.17	3.20	16.07	15.91	16.01	2.30	15.44	1.16
MnO	.47	.47	.07	.05	.43	.08	.14	.39	.04	.67	.06	.03	.42	.33	.46	.03	.40	.02
NiO	.09	.10	.12	.15	.00	.00	.00	.00	.64	.02	.64	.60	.10	.15	.04	.25	.16	.11
MgO	13.59	13.78	17.40	19.59	13.80	17.37	19.59	13.74	53.75	53.24	53.44	53.36	13.46	14.33	14.10	40.03	14.56	33.72
CaO	.02	.03	24.32	12.71	.00	24.41	12.81	.02	.04	.01	.03	.01	.00	.02	.02	.03	.01	.00
Na2O	.00	.00	.00	.00	.00	.00	.00	.00	.00	.00	.00	.00	.00	.00	.00	.00	.00	.00
K2O	.00	.00	.00	.00	.00	.00	.00	.00	.00	.00	.00	.00	.00	.00	.00	.00	.00	.00

NI-FE METAL

	#1	#2	#3	#4	#5	#18	#2B
S	.03	.00	.00	.01	.01	.01	.00
Ni	73.34	73.60	73.75	69.45	67.23	75.50	66.05
Fe	24.04	23.98	23.00	27.24	30.30	21.56	29.28
Cu	.26	.22	.11	.00	.00	.59	.03
Zn	.01	.08	.10	.05	.09	.00	.00

UVAROVITE (1-34, 1 (1-34, 1B-6B))

	#1	#2	#3	#4	#5	#6	#7	#8	#9	#10	#11	#12	#13	#14	#15	#16	#17	#18	#19	#20
	UV	UV	UV	UV	DIOP	DIOP	DIOP	DIOP	UV	UV	UV	UV	AMPH	AMPH	DIOP	DIOP	AMPH	AMPH	AMPH	AMPH
Si02	37.79	37.78	37.55	36.08	53.92	54.21	54.48	54.32	38.12	38.30	38.98	38.47	57.32	57.42	54.61	54.03	57.37	56.89	56.44	55.58
Ti02	.41	.39	.36	.41	.06	.04	.01	.02	12.95	14.24	13.64	13.18	.00	.00	.05	.00	.00	.00	.00	.01
Al2O3	10.99	11.01	10.98	11.06	2.04	1.88	1.28	1.97	12.95	14.24	13.64	13.18	.00	.06	1.48	.33	.43	.32	.45	.00
Fe2O3	13.44	13.44	13.06	12.87	2.08	1.55	1.76	1.24	10.36	9.17	8.93	9.65	.00	.00	.00	.00	.00	.00	.00	.00
Cr2O3	.00	.00	.00	.00	.00	.00	.00	.00	.00	.00	.00	.00	.00	.00	1.83	2.76	.00	.06	.08	.59
V2O5	2.53	2.37	2.34	2.60	4.66	4.87	4.45	4.37	2.52	2.56	2.64	2.39	.00	.00	.00	.00	.00	.00	.00	.00
FeO	.39	.37	.39	.44	.19	.18	.18	.20	.56	.58	.58	.57	.13	4.36	4.41	5.31	4.56	6.67	6.30	10.41
MnO	.00	.00	.00	.00	.00	.00	.00	.00	.00	.00	.00	.00	.00	.12	.21	.35	.11	.26	.21	.51
MgO	.00	.02	.03	.03	12.70	13.14	13.41	1.62	.02	.02	.65	.03	.00	.00	.00	.00	.00	.00	.00	.00
CaO	34.57	34.68	34.73	34.56	21.74	21.83	22.38	22.85	35.09	35.28	34.85	34.98	13.19	21.64	13.64	13.21	21.20	19.77	19.80	16.86
Na2O	.02	.00	.00	.00	1.81	1.58	1.54	1.62	.00	.00	.00	.00	.04	13.16	22.27	23.32	15.27	13.15	12.82	12.68
K2O	.00	.00	.00	.00	.00	.00	.00	.00	.00	.00	.10	.00	.02	.02	1.61	1.12	1.10	.06	.05	.09
Total	100.14	100.06	99.41	100.05	99.17	99.26	99.49	87.91	99.84	100.33	100.54	100.01	96.28	96.42	100.09	100.41	97.07	97.21	96.19	97.12

	#21	#22	#23	#24	#25	#26	#27	#28	#29	#30	#31	#32	#33	#34	#1B	#2B	#3B	#4B	#5B	#6B
	DIOP	DIOP	DIOP	DIOP	RB	RB	KSPRR	KSPRR	RB	RB	CHR	CHR	CHR	CHR	CHR	UV	UV	UV	DIOP	DIOP
Si02	55.40	54.65	54.62	54.21	68.16	68.34	62.07	61.54	68.46	68.20	.04	.06	.04	.07	.03	37.22	37.30	36.92	53.76	56.19
Ti02	.01	.02	.05	.00	.00	.00	.00	.00	.00	.00	.02	.08	.02	.03	.01	.47	.37	.35	.04	.02
Al2O3	.36	1.61	1.69	.43	19.82	19.75	17.00	15.87	19.66	19.86	20.87	20.42	19.84	21.54	19.01	9.31	9.50	10.19	1.65	.52
Fe2O3	2.88	1.63	1.50	.00	.00	.00	.00	.00	.00	.00	.00	.00	.00	.00	.00	.00	.00	.00	.00	.00
Cr2O3	.00	.00	.00	.00	.00	.00	.00	.00	.00	.00	47.32	47.35	47.17	46.65	45.77	13.66	13.54	12.47	1.23	.00
V2O5	5.60	4.66	5.02	5.19	.06	.03	.67	.90	.00	.00	.18	.21	.20	.00	.00	.00	.00	.00	.00	.00
FeO	.32	.27	.25	.26	.00	.00	.00	.00	.05	.06	20.41	20.05	20.24	17.61	19.39	1.92	1.83	1.94	3.70	.60
MnO	.00	.00	.00	.00	.00	.00	.00	.00	.00	.00	.20	.19	.18	.14	.33	.43	.46	.46	.22	.07
NiO	.00	.00	.00	.00	.00	.00	.00	.00	.00	.00	.09	.09	.10	.09	.09	.01	.00	.00	.03	.00
MgO	12.78	13.61	13.34	13.47	.00	.00	.00	.00	.00	.00	11.89	11.80	11.60	13.45	12.09	.00	.02	.02	13.59	17.89
CaO	22.88	22.59	22.59	22.99	.27	.21	1.61	1.84	.27	.22	.03	.19	.36	34.74	22.02	34.53	34.56	34.74	22.55	25.03
Na2O	1.16	1.54	1.44	1.19	11.64	11.49	.20	.21	11.49	11.62	.00	.00	.00	.00	.00	.00	.00	.00	.00	.00
K2O	.06	.00	.02	.06	.11	.11	13.51	13.28	.16	.08	.00	.00	.00	.00	.00	.00	.00	.00	.00	.00
Total	99.42	100.58	100.52	100.71	100.06	99.91	97.22	95.85	100.12	100.06	101.05	100.42	99.75	99.90	96.68	97.55	97.58	97.09	96.78	99.33

PIT-6-1

	#1	#2	#3	#4	#5	#6	#7	#8	#9	#10	#11	#12	#13	#14	#15	#16	#17	#18
SiO2	41.09	41.06	40.85	46.67	.09	47.36	.09	.00	.02	.01	.01	.00	.00	.13	.00	38.97	36.91	43.02
TiO2	.00	.00	.00	.50	.26	.47	.25	.14	.15	.17	.16	.17	.18	.17	.18	.00	.00	.00
Al2O3	.02	.03	.00	8.77	13.78	7.92	13.64	15.04	15.47	15.61	15.25	15.90	19.21	23.53	17.05	22.49	22.46	31.02
Fe2O3	.57	.41	.00	.00	.00	.00	.00	.00	53.98	53.66	54.77	53.40	50.38	46.06	.00	.00	.00	.00
Cr2O3	.00	.00	.00	3.11	55.95	2.56	55.72	54.46	53.98	53.66	54.77	53.40	50.38	46.06	.00	.00	.00	.00
V2O3	4.22	4.46	4.26	2.03	17.97	1.81	18.32	18.10	17.87	17.92	18.62	17.55	16.97	16.19	17.25	1.57	3.21	1.41
FeO	.06	.05	.06	.09	.34	.05	.41	.11	.07	.11	.11	.15	.16	.21	.13	8.50	8.92	3.79
MnO	1.01	.90	.97	.24	.24	.23	.21	.13	.15	.15	.14	.15	.16	.11	.16	.07	.00	.00
MgO	54.08	53.62	53.74	19.56	12.31	20.34	12.56	12.95	12.33	12.96	12.55	12.74	13.76	14.86	13.17	28.62	22.97	11.11
CaO	.00	.00	.02	11.75	.09	11.29	.05	.00	.00	.00	.01	.00	.00	.00	.00	.00	.00	.00
Na2O	.00	.00	.00	.00	.00	.00	.00	.00	.00	.00	.00	.00	.00	.00	.00	.00	.00	.00
K2O	.00	.00	.00	.00	.00	.00	.00	.00	.00	.00	.00	.00	.00	.00	.00	.00	.00	.00

	#35	#36	#37	#38	#39	#40	#41	#42	#43	#44	#45	#46	#47	#48	#49	#50	#51	#52
SiO2	38.67	38.86	38.82	38.62	38.91	42.77	44.83	42.67	42.00	37.64	55.81	54.06	31.41	39.22	35.28	27.02	61.52	54.44
TiO2	.00	.00	.00	.00	.00	.02	.02	.00	.05	.05	.03	.03	.00	.02	.00	.00	.00	.00
Al2O3	30.95	33.75	32.59	33.63	33.25	36.98	38.10	24.75	24.38	29.18	.76	2.59	15.18	13.62	9.86	21.11	23.80	21.43
Fe2O3	.00	.00	.00	.00	.00	.00	.00	.00	.00	.00	.00	.00	.00	.00	.00	.00	.00	.00
Cr2O3	.00	.00	.00	.00	.00	.00	.00	.05	.03	.06	.03	.03	.00	.01	.00	.02	.00	.00
V2O3	.02	.00	.00	.00	.02	.00	.00	.00	.00	.00	.00	.00	.00	.00	.00	.00	.00	.00
FeO	3.29	.43	.73	.15	.23	.79	.23	.41	.16	5.27	3.86	3.94	6.95	5.74	1.71	11.89	.03	.20
MnO	.00	.00	.06	.00	.00	.10	.00	.06	.05	.24	.66	2.05	.30	.43	.03	1.29	.00	.00
NiO	.00	.00	.00	.00	.00	.00	.00	.00	.00	.00	.00	.00	.00	.00	.00	.00	.00	.00
MgO	.06	.07	.83	.05	.15	1.11	.06	.00	.00	.07	21.55	19.44	30.64	25.44	37.01	24.64	.00	.00
CaO	23.55	22.26	23.60	22.73	24.22	1.11	.06	23.43	26.55	23.49	12.52	12.97	30.64	25.44	37.01	24.64	5.08	.04
Na2O	.00	.00	.00	.00	.00	.07	.10	.00	.02	.08	.07	.40	.00	.00	.00	.00	8.71	.45
K2O	.00	.00	.00	.00	.00	9.97	11.28	1.01	.07	.08	.13	.30	.10	4.69	.00	.03	.06	11.43
BaO	.00	.00	.00	.00	.00	.00	.00	.00	.00	.00	.00	.00	.00	.00	.00	.00	.05	12.82

PIT-G-IR(CONTINUED)

	#19	#20	#21	#22	#23	#24	#25	#26	#27	#28	#29	#30	#31	#32	#33	#54	#55	#57	#58	#59	#60	#61	#62	#63	#64	#65	#66	#67	#68	#69	#70	#71			
	GARN	GARN	GARN	GARN	GARN	GARN	GARN	GARN	GARN	GARN	GARN	GARN	GARN	GARN	GARN	KSPAR	PLAG	PLAG	PLAG	PLAG	PREH	PREH	KSPAR	PREH	PREH	PREH	BIO	BIO	PREH	GARN	GARN	GARN	GARN		
SiO2	39.33	38.49	38.83	38.76	38.71	38.91	38.79	38.88	38.82	38.62	38.44	38.80	38.86	38.70	38.54	55.69	60.71	59.43	61.49	61.85	43.88	43.01	54.38	42.97	42.34	37.65	36.85	43.38	38.34	38.04	37.98	37.80			
TiO2	.00	.00	.00	.00	.00	.00	.00	.00	.00	.00	.00	.00	.00	.00	.00	.00	.00	.00	.00	.00	.00	.00	.00	.00	.00	.00	.00	.00	.00	.00	.00	.00	.00	.00	
Al2O3	22.77	22.78	22.45	22.49	22.40	22.45	22.39	22.40	22.70	22.35	22.23	22.57	22.90	22.31	22.65	20.82	23.78	25.09	23.89	23.51	24.14	24.05	21.46	24.36	24.32	14.87	14.00	24.38	20.07	21.28	21.55	22.18	22.00		
Fe2O3	.00	.00	.00	.00	.00	.00	.00	.00	.00	.00	.00	.00	.00	.00	.00	.00	.00	.00	.00	.00	.00	.00	.00	.00	.00	.00	.00	.00	.00	.00	.00	.00	.00	.00	
Cr2O3	.00	.00	.00	.00	.00	.00	.00	.00	.00	.00	.00	.00	.00	.00	.00	.00	.00	.00	.00	.00	.00	.00	.00	.00	.00	.00	.00	.00	.00	.00	.00	.00	.00	.00	.00
U2O3	.02	.00	.02	.00	.04	.00	.00	.02	.01	.00	.00	.02	.00	.00	.00	.00	.00	.00	.00	.00	.00	.00	.00	.00	.00	.00	.00	.00	.00	.00	.00	.00	.00	.00	.00
FeO	1.84	1.91	1.71	1.53	1.62	1.66	1.45	1.61	1.57	2.09	1.71	1.67	1.76	1.98	1.75	1.84	1.91	1.71	1.53	1.62	1.66	1.45	1.61	1.57	2.09	1.71	1.67	1.76	1.98	1.75	1.84	1.91	1.85		
MnO	9.62	10.19	9.92	7.49	6.85	5.97	6.68	5.55	7.17	8.53	8.82	7.29	7.92	8.26	4.78	10.19	9.92	7.49	6.85	6.85	5.97	6.68	5.55	7.17	8.53	8.82	7.29	7.92	8.26	4.78	10.19	9.92	15.95		
NiO	.00	.00	.00	.00	.00	.00	.00	.00	.00	.00	.00	.00	.00	.00	.00	.00	.00	.00	.00	.00	.00	.00	.00	.00	.00	.00	.00	.00	.00	.00	.00	.00	.00	.00	.00
MgO	.07	.06	.04	.03	.09	.05	.05	.07	.04	.00	.00	.04	.00	.00	.00	.00	.00	.00	.00	.00	.00	.00	.00	.00	.00	.00	.00	.00	.00	.00	.00	.00	.00	.00	.00
CaO	27.20	26.66	26.91	29.83	30.35	31.22	30.51	31.53	30.05	28.26	28.18	29.78	29.46	28.81	32.30	27.20	26.66	26.91	29.83	30.35	31.22	30.51	31.53	30.05	28.26	28.18	29.78	29.46	28.81	32.30	27.20	26.66	26.91	29.83	
Na2O	.00	.00	.00	.00	.00	.00	.00	.00	.00	.00	.00	.00	.00	.00	.00	.00	.00	.00	.00	.00	.00	.00	.00	.00	.00	.00	.00	.00	.00	.00	.00	.00	.00	.00	.00
K2O	.00	.00	.00	.00	.00	.00	.00	.00	.00	.00	.00	.00	.00	.00	.00	.00	.00	.00	.00	.00	.00	.00	.00	.00	.00	.00	.00	.00	.00	.00	.00	.00	.00	.00	.00
BaO	11.16	.07	.03	.06	.03	.04	.06	10.77	.04	.07	9.78	9.11	.05	.02	.03	11.16	.07	.03	.06	.03	.04	.06	10.77	.04	.07	9.78	9.11	.05	.02	.03	.04	.06	.03	.04	.06

CR-PIT-2

	#1	#2	#3	#4	#5	#6	#7	#8	#9	#10	#11	#12	#13
	CHR	CHR	CHR	CHR	CHR	CHR	CHR	CHR	CHR	CHR	SERP	SERP	SERP
S102	.04	.03	.04	.04	.15	.10	.04	.37	.11	.10	39.86	42.59	48.92
T102	.14	.12	.12	.03	.55	.52	.04	.13	.15	.11	.00	.00	.00
Al2O3	16.43	16.11	16.06	17.66	.34	1.17	17.90	2.46	4.06	3.11	.73	.52	.74
Fe2O3	.00	.00	.00	.00	.00	.00	.00	.00	.00	.00	.00	.00	.00
Cr2O3	53.78	53.10	53.91	51.38	47.76	48.03	51.24	59.80	60.26	60.12	.40	.29	.14
V2O3	.07	.14	.09	.05	.16	.14	.08	.09	.13	.15	.01	.04	.00
FeO	16.79	16.99	17.15	19.10	46.38	46.12	19.19	33.03	31.48	29.98	12.38	3.81	4.05
MnO	.16	.11	.08	.16	1.72	1.49	.12	1.10	.71	.61	.21	.08	.07
NiO	.07	.08	.09	.01	.08	.10	.00	1.08	.07	.09	.12	.31	.16
MgO	13.39	13.85	13.74	11.97	.29	.59	11.78	1.93	4.44	4.64	32.99	39.12	37.64
CaO	.00	.00	.00	.18	.00	.22	.11	.12	.09	.05	.02	.05	.00
Na2O	.00	.00	.00	.00	.00	.00	.00	.00	.00	.00	.00	.00	.00
K2O	.00	.00	.00	.00	.00	.00	.00	.00	.00	.00	.00	.00	.00

SULFIDES

	#1	#2	#3	#4	#5	#6	#7	#8	#9	#10	#11	#12	#13
	CHR	CHR	CHR	CHR	CHR	CHR	CHR	CHR	CHR	CHR	SERP	SERP	SERP
S	33.00	34.41	33.20	18.32	41.59	39.61	39.07	36.07	32.88	33.35	33.19	39.77	38.44
Ni	38.48	38.37	36.36	30.50	32.57	27.05	26.21	32.78	38.01	37.59	37.73	27.29	28.01
Fe	27.72	27.93	27.77	15.98	21.43	26.60	27.57	27.07	27.12	27.57	27.48	27.28	28.70
Cu	.00	.05	.02	.00	.00	.00	.00	.08	.03	.00	.00	.00	.00
Zn	.03	.00	.02	.00	.00	.01	.00	.00	.06	.00	.00	.04	.07
TOTAL	99.23	100.76	99.37	64.40	95.59	93.27	92.85	96.00	98.10	98.31	98.40	94.38	97.22



CR-PIT-2 (CONTINUED)

	#14	#15	#18	#28	#38	#48	#58	#68	#78	#88	#98	#108	#118	#128	#148	#158
	SERP	DOL	CHR	CHR	CHR	SERP	SERP	SERP	SERP	SERP	CHR	CHR	CHR	CHR	CHR	CHR
SiO2	39.40	.06	.05	.02	.01	42.88	42.67	37.07	44.60	32.52	.03	.03	.02	.04	.02	.04
TiO2	.00	.00	.15	.15	.14	.00	.02	.02	.01	.02	.12	.13	.13	.13	.13	.11
Al2O3	1.63	.00	14.32	14.81	14.72	3.39	.40	1.04	1.13	14.41	15.15	15.29	15.01	15.16	14.70	14.66
Fe2O3	.45	.00	.00	.00	.00	.00	.00	.00	.00	.00	.00	.00	.00	.00	.00	.00
Cr2O3	.05	.00	53.75	53.58	52.80	1.50	.80	.20	.40	2.70	52.49	52.95	52.66	52.39	53.55	52.88
V2O5	10.02	1.84	15.29	15.04	15.07	3.68	4.16	2.48	4.95	.80	.00	.00	.00	.00	.00	.00
FeO	.13	.56	.37	.44	.38	.04	.05	.03	.06	.00	.30	.32	.34	.28	.36	.35
MnO	.12	.01	.09	.14	.05	.12	.11	.17	.36	.08	.12	.08	.09	.13	.05	.04
MgO	34.02	19.94	14.55	14.76	14.62	38.25	38.54	31.55	35.04	34.78	15.13	15.47	15.20	15.37	14.19	14.25
CaO	.04	28.14	.01	.00	.02	.01	.03	.07	.17	.03	.00	.00	.00	.00	.01	.01
Na2O	.00	.00	.00	.00	.00	.00	.00	.00	.00	.00	.00	.00	.00	.00	.00	.00
K2O	.00	.00	.00	.00	.00	.00	.00	.00	.00	.00	.00	.00	.00	.00	.00	.00

SULFIDES

	#48	#58	#68	#78	#88	#98	#108	#118	#128	#138	#148	#158	#168
S	40.01	32.98	33.08	33.28	1.14	33.28	33.11	33.35	33.29	3.71	3.68	36.76	38.67
Ni	27.70	37.64	33.39	37.81	9.54	38.03	38.36	38.30	38.37	8.87	10.01	24.76	28.78
Fe	26.67	27.65	27.80	27.55	40.15	27.20	27.78	27.42	28.14	41.89	41.01	29.60	28.86
Cu	.00	.00	.00	.00	.00	.00	.00	.00	.02	.00	.00	.00	.07
Zn	.00	.01	.00	.00	.00	.01	.00	.06	.00	.04	.02	.00	.00
TOTAL	94.38	98.28	94.27	98.68	50.83	98.52	99.25	99.13	99.82	54.51	54.72	91.12	93.38

APPENDIX II

CIPW NORMS CALCULATED FROM ANALYSES PRESENTED IN TABLE 13

APPENDIX II : CIPW NORMS CALCULATED FROM ANALYSES PRESENTED IN TABLE 13

	STER-GT-1Q	STER-GT-1B	STER-GT-1Z	UVAPOWITE	STER-G-3B	STER-FG-1	STER-FG-2	STER-FG-4	STER-44
APATITE	.03	.05		.10	.09	.03	.06	.06	.19
ILMENITE	.30	.06		.16	.21	.02	.29	.07	.21
MAGNETITE	2.32	1.19		2.40	.92	2.47	2.30	2.42	.69
ORTHOCLASE	.27	19.81		.79	9.00	.07	.07	.14	11.84
ALBITE	.09	.09		1.84	74.12	.10	.10	.10	48.67
ANORTHITE	17.91	20.96		3.06	5.00	1.32	1.20	2.39	3.57
DIOPSIDE	.00	.00		53.55	3.07	.23	2.86	5.81	.00
HYPERSTHENE	16.53	10.73		29.15	5.17	24.64	27.32	18.02	.00
OLIVINE	56.17	27.46		.00	.00	71.12	65.81	70.99	.00
NEPHELINE	.00	.00		.00	.00	.00	.00	.00	.00
ACMITE	.00	.00		.00	.00	.00	.00	.00	.00
CORUNDUM	6.39	19.64		.00	.00	.00	.00	.00	.00
QUARTZ	.00	.00		8.95	2.40	.00	.00	.00	.00

	STER-1A	STER-1B	PIT-B	CODD-21A	CODD 0+50B	CODD 2+65	STER-30D	STER-46	STER-49
APATITE	.03	.03		.16	.14	.14	.14	.03	.19
ILMENITE	.29	.02		.15	.46	.33	.33	.02	.21
MAGNETITE	.90	1.64		.38	3.91	2.28	2.07	2.07	.69
ORTHOCLASE	.07	.28		1.01	3.53	4.48	.07	.07	11.84
ALBITE	.10	.10		58.93	57.60	53.36	.10	.10	48.67
ANORTHITE	.00	.52		1.34	7.51	7.62	.61	.61	3.57
DIOPSIDE	.00	.00		.00	12.27	2.09	.00	.00	.00
HYPERSTHENE	22.17	6.65		.49	10.84	5.77	45.32	45.32	1.88
OLIVINE	61.45	90.38		.00	.00	.00	51.30	51.30	.00
NEPHELINE	.00	.00		.00	.00	.00	.00	.00	.00
ACMITE	.00	.00		.00	.00	.00	.00	.00	.00
CORUNDUM	15.02	.39		.83	.00	.00	.49	.49	.72
QUARTZ	.00	.00		36.71	3.75	23.94	.00	.00	32.24